in vivo *28*: 147-172 (2014)

Differences in Irradiated Lung Gene Transcription Between Fibrosis-Prone C57BL/6NHsd and Fibrosis-resistant C3H/HeNHsd Mice

RONNY KALASH†, HEBIST BERHANE, JEREMIAH AU, BYUNG HAN RHIEU, MICHAEL W. EPPERLY, JULIE GOFF, TRACY DIXON, HONG WANG, XICHEN ZHANG, DARCY FRANICOLA, ASHWIN SHINDE and JOEL S. GREENBERGER

Department of Radiation Oncology, University of Pittsburgh Cancer Institute, Pittsburgh, PA, U.S.A.

Abstract. *Background/Aim: We compared pulmonary irradiation-induced whole-lung, gene transcripts over 200 days after 20 Gy thoracic irradiation in female fibrosis-prone C57BL/6NHsd mice with fibrosis-resistant C3H/HeNHsd mice. Materials and Methods: Lung specimens were analyzed by real time polymerase chain reaction (rt-PCR) and changes over time in representative gene transcript levels were correlated with protein levels using western blot. Results: C3H/HeNHsd mice showed a significantly longer duration of elevation of gene transcripts for stress-response genes nuclear factor kappa-light-chain-enhancer of activated B cells (Nfkb), nuclear factor (erythroid-derived 2)-like 2 (Nrf2), transcription factor SP1 (SP1), activator protein 1 (AP1), radioprotection gene manganese superoxide dismutase (Sod2), and endothelial cell-associated genes von Willebrand factor (Vwf) and vascular endothelial growth factor (Vegf). C57BL/6NHsd mice showed acute elevation then down-regulation and a second elevation in gene transcripts for Nfkb, connective tissue growth factor (Ctgf), insulin-like growth factor-binding protein 7 (Igfbp7), tumor necrosis factor-alpha (Tnfa) Ctgf, Igfbp7, Tnfa, collagen 1a, and toll like receptor 4 (Tlr4). There were reciprocal patterns of elevation and decrease in levels of transcripts for epigenetic reader proteins bromodomain coding protein 1 (Brd1)Brd2,-3, and -4 between mouse strains. Conclusion: Regulatory pathways linked to radiation pulmonary fibrosis may identify new targets for mitigators of radiation-induced fibrosis.*

†Presented at the ASTRO 55th Annual Meeting, Atlanta, Georgia 22-25/9/2013.

Correspondence to: Joel S. Greenberger, MD, Professor and Chairman, Department of Radiation Oncology, University of Pittsburgh Cancer Institute, UPMC Cancer Pavilion, 5150 Centre Avenue, Rm. 533, Pittsburgh, P A 15232, U.S.A. Tel: +1 4126473602, Fax: +1 4126476029, e-mail: greenbergerjs@upmc.edu

Key Words: Radiation fibrosis, genetic, epigenetic, bone marrow.

A major dose-limiting complication of thoracic radiotherapy is lung damage (1-15). Acute radiation pneumonitis is characterized by endothelial cell swelling, alveolar transudates, and local pulmonary, as well as circulatory, elevation of inflammatory cytokines, prominently Interleukin-1 (*Il1*), *Il6*, *Il10*, Transforming growth factor beta (*Tgfb*), and *Tnfa* (4, 7-10, 16). Treatment with non-steroidal, or steroid anti-inflammatory agents may ameliorate symptoms of radiation pneumonitis, which is dependent upon the volume of irradiated lung, fraction size, and total dose (1, 2). Not all patients who suffer radiation pneumonitis go on to develop late pulmonary fibrosis, suggesting distinct differences in the pathophysiology between these two types of lesions (4, 12, 15, 17).

A valuable model system in which to dissect the mechanisms of late pulmonary fibrosis is the fibrosis-prone C57BL/6NHsd mouse compared to the pneumonitis-prone, but fibrosis-resistant C3H/HeNHsd mouse (17, 18-21). C3H/HeNHsd mice are intrinsically radiosensitive to total-body irradiation (TBI), and display radiation dose-dependent life shortening (18-22) and radiation pneumonitis. In contrast, C57BL/6NHsd mice are relatively radioresistant to TBI, demonstrating a brief interval of acute radiation pneumonitis followed by a period during which pulmonary histopathology is indistinguishable from unirradiated mice, then develop distinct organizing alveolitis (fibrosis) (18), involving proliferation of both intrinsic lung fibroblasts and bone marrow origin fibroblast progenitors, which migrate to sites of fibrosis (15, 18, 23, 24).

Recent studies with C57BL/6NHsd mice (24, 25) demonstrated an initial increase in expression of genes for promoter-binding proteins, stress response, and inflammatory cytokine genes, which returned to normal levels during a

0258-851X/2014 $2.00+.40

subsequent latent period, followed by elevation of many of the same gene transcripts and proteins, at the time of first detection of histopathological fibrosis (24). Transcripts for endothelial cell-related genes including *Vwf* and *Vegf* remained elevated in irradiated lungs of C57BL/6NHsd mice, indicating a persistent irradiation damage response (24, 25). The genetic and molecular biological determinants that initiate pulmonary fibrosis in C57BL/6NHsd, but not C3H/HeNHsd mice are not known.

In the present study, we quantitated post-thoracic irradiation levels of 25 representative gene transcripts in the irradiated lungs of C57BL/6NHsd, compared to C3H/HeNHsd mice. These transcripts were organized into six groups based on either their published involvement in radiobiological responses of cells and tissues to ionizing irradiation or data showing their association with lung fibrosis that was attributable to other causes. The first group consisted of representative inflammatory response genes for proteins known to be acutely elevated after thoracic irradiation of C57BL/6J/NHsd mice including: *Nfkb, Nrf2, Sp1*, and *Ap1*. A second group of gene transcripts was chosen based on endothelial cells, which have been implicated in early irradiation responses in several organs, including the intestine; these included *Vwf, Vegf, Ctgf,* and *Il6* (26). A third group of transcripts included those for gene products known to be associated with initiation of fibrosis or found elevated in fibrotic areas of the lungs of patients with lung transplant rejection or those having lung resection for scleroderma lung including maganese superoxide dismutase (*Sod2*), *Il1, Tnfα, Lysl Ox, Igfbp7*, and *Tgfb* (27-28). As a fourth indicator of the fibrosis response, we measured levels of RNA transcripts for collagen 1a, known to be a dominant part of the fibrotic lung in C57BL/6NHsd mice (24-25). A fifth group included Toll-like receptors (*Tlr*) 1-7 known to be up-regulated during the inflammatory response (29, 30). An initial inflammatory response has been reported to occur in lungs of both fibrosis-prone and fibrosis-resistant mice (24, 31). Finally, a sixth group of transcripts included bromodomain epigenetic reader protein *Brd1-4* (32, 33).

Materials and Methods

Thoracic radiation of mice. C57BL/6NHsd and C3H/HeNHsd mice were obtained from Harlan Laboratories (Indianapolis, IN, USA) and housed five per cage according to University of Pittsburgh Institutional Animal Care and Use Committee (IACUC) protocols. Mice were irradiated to the thoracic cavity with shielding of the head and neck, abdomen, and lower body according to published methods (34). Female C57BL/6NHsd mice received 20 Gy and groups of female C3H/HeNHsd mice received 14, 16.5, or 20 Gy irradiation to the thoracic field and were then maintained according to IACUC-directed laboratory conditions. Mice were sacrificed at serial time points after thoracic irradiation including pre-irradiation, days 2, 7, 14, 28, 60, 100, 125, 150 and 200 post-irradiation. A log-rank test was used to statistically analyze the survival curves after *in vivo* irradiation.

Measurement of levels of gene transcripts for irradiation-inducible transcription factors, growth factors, inflammatory cytokines, adhesion molecules, and radiation-protective enzymes by real-time polymerase chain reaction (RT-PCR). RNA was extracted from mouse lung using the TRIzol reagent (Invitrogen, Carlsbad, CA, USA) following the manufacturer's instructions, quantified using a spectrophotometer, and stored at −80˚C (34). Reverse transcription of 2 μg of total RNA to complementary DNA (cDNA) was accomplished using the High Capacity cDNA Reverse Transcription Kit (Applied Biosystems, Foster City, CA, USA) according to the manufacturer's protocol.

In subsequent steps, expression of specific RNA moieties included: *Gpdh* (Gen-Bank: NM_008084.2), *Gusb* (Gen-Bank: NM_010368.1), *Nfkb* (Gen-Bank: NM_199267.2), *Tnfa* (Gen-Bank: NM_013693.2), *Nrf2* (Gen-bank: NM_010902.3) (21), *Nfkb* (Gen-Bank: NM_008689.2), Jun (Gen-Bank: NM_010591.2), *Sp1* (Gen-Bank: NM_013672.2), *Ap1* (Gen-Bank: NM_001243043.1), *Lysl Ox* (Gen-Bank: NM_001178102.1), *Tgfb1* (Gen-Bank: NM_011577.1), *Vegfa* (Gen-Bank: NM_001025250.3), *Il1a* (Gen-Bank: NM_010554.4), *Fgf1* (Gen-Bank: NM_010197.3), *Ifng* (Gen-Bank: NM_008337.3), *Il6* (Gen-Bank: NM_031168.1), *Fap* (Gen-Bank: NM_007986.2), *Vwf* (Gen-Bank: NM_011708.3), *Ctgf* (Gen-Bank: NM_010217.2), *Sod2* (Gen-Bank: NM_013671.3), *Igfbp7* (Gen-Bank: NM_001159518.1) and epigenetic reader proteins *Brd1* (Gen-Bank: AK149714.1), *Brd2* (Gen-Bank: AB010246.1), *Brd3* (Gen-Bank: AB206708.2), and *Brd4* (Gen-Bank: AF273217.1). collagen 1a (Gen-Bank: AK132180.1). Each was quantitated by RT-PCR. Ninety-six-well plates were prepared with 10 μl of Taqman Gene Expression Master mix, 5 μl of RNase-free water, 1 μl of the corresponding Taqman Gene Expression probe, and 4 μl of cDNA (totaling 2 μg cDNA) using the Eppendorf epMotion 5070 automated pipetting system (Eppendorf, Westbury, NY). The cDNA was amplified with 40 cycles of 95˚C (denaturation) for 15 s and 60°C (annealing and elongation) for 1 min using the Eppendorf Realplex2 Mastercycler (17, 35).

Data for each gene transcript were normalized by calculating the differences (ΔCt) from the Ct of *Gusb* and Ct of target genes. The relative increase or decrease in expression was calculated by comparing the reference gene with the target gene (ΔΔCt) and using the formula for relative expression ($=2^{\Delta\Delta Ct}$). Subsequently, ΔΔCt levels were compared and *p*-values were calculated using one-way ANOVA followed by Tukey's multiple comparison tests. The results were presented as the percentage increase in RNA above baseline levels which were adjusted to that of unirradiated C57BL/6NHsd and C3H/HeNHsd mice (34). Baseline transcript levels were standardized to that of *Gpdh*.

Western analysis for protein expression in irradiated mouse lungs. To determine levels of representative proteins *Sod2, Nfkb, Brd4*, and collagen-1 in C3H/HeNHsd lung tissue post 20 Gy thoracic irradiation, lung tissue was taken at acute (day 2), latent (day 60), and late (day 150) times and lysed in NP-400 buffer [50 mM Tris, pH 7.8, 10 mM ethylenediaminetetaacetic acid (EDTA), 150 mM NaC1, 1 mM phenylmethylsulfonyl fluoride (PMSF), 1% NP-40, and a protease inhibitor cocktail tablet (Roche Diagnostics, Indianapolis, IN, USA)]. Protein samples were separated in 15% polyacrylamide gels by electrophoresis and transferred to nitrocellulose membranes. Primary antibody to MnSOD (Novus Biologicals, Littleton, CO, USA) or α-tubulin (Sigma Aldrich, St. Louis, MO, USA) antibody were used. Horseradish peroxidase antirabbit or anti-mouse secondary antibody (Promega, Pittsburgh, PA, USA) was then applied and membranes developed with Super Signal West Dura ECL (Thermo Scientific, Rockford, IL, USA). Antibodies were obtained from Santa Cruz Biochemical Laboratories, Santa Cruz, CA, USA. Antibodies used were anti-*Sod2* (ab13533), anti-*Nfkβ* p65(ab16502), anti-collagen 1 (ab34710), and anti-*Brd4* [EPR5150(2)] (ab128874) from Abcam, Cambridge, MA, USA. For quantification of levels of proteins, band densities were quantified with Image J (National Institutes of Health, www.rsbweb.nih.gov/ij), previously as published (34).

In vivo imaging of coat changes post-thoracic irradiation. Groups of C3H/HeNHsd and C57BL/6NHsd mice were irradiated to the thorax to 20 Gy. At 47 days post-irradiation, when C57BL/6NHsd mice typically show graying of fur in irradiated fields (24), two isoflurane-anesthetized mice from each strain were imaged using a Xenogen IVIS 200 Imaging System (Advanced Molecular Vision Ltd, Lincolnshire, United Kingdom).

Serial imaging of luc+ bone marrow stromal cells. C3H/HeNHsd mice were injected intraperitoneally (*i.p.*) at each of several time points after 20 Gy thoracic irradiation with 1×10^6 luc+ bone marrow stromal cells from a C3H/HeNHsd luc+ stromal cell line. Following injection with D-luciferin (Gold Biotechnology, St. Louis, MO, USA), mice were imaged at serial timepoints using a Xenogen IVIS 200 Imaging System and the bioluminescent signal for each mouse was quantitated. As controls for pulmonary migration of luc+ bone marrow stromal cells in C3H/HeNHsd mice, C57BL/6NHsd mice received 20 Gy thoracic irradiation and were injected *i.p.* with 1×10^6 C57BL/6NHsd luc+ bone marrow stromal cells from a C57BL/6 luc+ stromal cell line (24). Mice were imaged and the bioluminescent signal for each mouse was quantified. Late-phase bioluminescence in C3H/HeNHsd mice was compared to late-phase bioluminescence C57BL/6NHsd mice using Student's t-test (24).

Pulmonary histopathology. Lungs from irradiated and unirradiated control C3H/HeNHsd and C57BL/6NHsd mice were removed, embedded in OCT and frozen. Frozen sections were stained with hematoxlyn and eosin (H&E), Masson's trichrome (for collagen), and antibody to leukocyte common antigen (CD45) (28). For CD45 immunostaining, sections were incubated with a monoclonal rat primary antibody to mouse CD45 (BD Pharmingen, San Jose, CA, USA), followed by a goat anti-rat Alexa Fluor 555 secondary antibody (Invitrogen, Grand Island, NY, USA).

Measurement of CpG promoter methylation. DNA was directly extracted from lung samples according to the manufacturer's instructions using the DNeasy Blood & Tissue Kit (Qiagen, Hilden, Germany). The percentage CpG promoter methylation was then measured using the EpiTect Methyl II PCR Assay (Qiagen). Briefly, 250 ng of isolated DNA was incubated in 26 μl of 5× restriction digestion buffer and methylation-sensitive/-dependent/null enzymes overnight at 37˚C, and then heat-inactivated for 20 min at 65˚C. Ninety-six-well plates were prepared with 12.5 μl of SYBR Green qPCR Master mix, 6.5 μl of RNase-free water, 1 μl of the corresponding EpiTect PCR Primer, and 5 μl of DNA digest. The DNA was then amplified with 40 cycles of 97˚C (denaturation) for 15 s and 72˚C (annealing and elongation) for 1 min using the Eppendorf Realplex2 Mastercycler (Eppendorf, Westbury, NY, USA). The fraction of methylated DNA for each gene promoter was calculated by normalizing the DNA amount to the amount of digestible DNA. The amount of digestible DNA was equal to the total amount of DNA (determined from the mock digest) minus the amount of DNA resistant to DNA digestion (determined from the double digest).

Statistics. Survival of thoracic-irradiated C3H/HeNHsd and C57BL/6NHsd mice was compared pairwise with the two-sided log-rank test.

For the comparison of gene transcript expression between the two mouse strains, data are summarized as mean±standard deviation in each group. For lungs from each mouse strain, expression of each of the 25 genes was compared against that at day 0 for each day after irradiation. We also compared the two mouse strains for each gene transcript level at each day.

For the analysis of mouse lung protein levels by western blot data, data were summarized as mean±standard deviation for the densitometry of each protein for each group. For each mouse strain and each of four representative proteins, values on each day were compared to day-0 values, which were set to 1, using the two-sided one-sample *t*-test. We also compared mouse strains for each gene product protein at each day, using the two-sided two-sample *t*-test. In all the above tests, *p*-values less than 0.05 were regarded as significant. As these were exploratory studies, *p*-values were not adjusted for multiple comparisons.

Results

C3H/HeNHsd mice are relatively sensitive to 20 Gy thoracic irradiation compared to C57BL/6NHsd mice. After 20 Gy thoracic irradiation, C57BL/6NHsd mice all survived to 125 days. In contrast, 20% of C3H/HeNHsd mice irradiated to 20 Gy died within seven days from acute pneumonitis ($p=0.0013$) (Figure 1). Following lower doses of 14.5 Gy or 16 Gy thoracic irradiation, all C3H/HeNHsd mice survived to 100 days (Figure 1).

Distinct gene expression patterns in irradiated C3H/HeNHsd compared to C57BL/6NHsd mouse lung. Levels of baseline expression of each of the 25 gene transcripts were first standardized using glucose phosphate dehydrogenase (GPDH) as a control (Table I). For 13 transcript levels, there was no significant difference between mouse strains. The levels of transcripts for nine genes: *vWF, VEGFa, TGFβ, TNFα, COL1a, TLR1, TLR4, Brd2*, and *Brd3* were higher in C57BL/6NHsd mouse lungs, and levels of three other gene transcripts: *CTGF, Lysl Ox*, and *TLR7* were higher in C3H/HeNHsd mouse lungs. After 14.5 Gy or 16 Gy thoracic irradiation to C3H/HeNHsd mice, transcript responses were similar to those of the 20-Gy irradiation group, and there was no detectable late histopathological evidence of pulmonary fibrosis in any of the groups of irradiated mice (data not shown). Despite early death of some C3H/HeNHsd mice irradiated with 20 Gy, we compared lung tissue responses to the known fibrosis-inducing dose of 20 Gy thoracic

Table I. *Comparison of baseline levels of gene transcripts between C57BL/6NHsd and C3H/HeNHsd whole lungs.*

Mouse Strain	NFKB	Nrf2	SP1	AP1	vWF
C57BL/6NHsd	38.55±1.27 (n=4)	25.60±0.63 (n=4)	9.93±0.87 (n=4)	15.70±0.88 (n=4)	39.53±1.06 (n=4)
C3H/HeNHsd	39.80±2.01 (n=4)	24.68±1.29 (n=4)	11.63±1.31 (n=4)	17.93±1.78 (n=4)	36.85±1.61 (n=4)
p-Value	0.3337	0.2451	0.0738	0.0661	0.0320
Mouse Strain	**VEGFa**	**FGF1**	**CTGF**	**IL6**	**SOD2**
C57BL/6NHsd	17.30±0.84 (n=4)	20.67±1.23 (n=4)	11.35±0.88 (n=4)	20.13±0.99 (n=4)	38.78±1.12 (n=4)
C3H/HeNHsd	15.48±1.04 (n=4)	19.33±0.69 (n=4)	14.33±1.22 (n=4)	21.20±1.68 (n=4)	35.95±2.03 (n=4)
p-Value	0.0342	0.1038	0.0076	0.3129	0.0511
Mouse Strain	**TGFb**	**Lysl Ox**	**IGFbp7**	**TNFa**	**Col1a**
C57BL/6NHsd	21.20±0.95 (n=4)	26.05±0.79 (n=4)	11.38±0.59 (n=4)	23.23±0.67 (n=4)	16.28±0.73 (n=4)
C3H/HeNHsd	19.03±0.92 (n=4)	27.28±0.61 (n=4)	12.33±0.66 (n=4)	21.05±0.85 (n=4)	14.93±0.51 (n=4)
p-Value	0.0166	0.0486	0.0747	0.0071	0.0226
Mouse Strain	**TLR1**	**TLR2**	**TLR4**	**TLR5**	**TLR6**
C57BL/6NHsd	15.35±0.48 (n=4)	20.60±0.74 (n=4)	23.10±0.79 (n=4)	11.45±1.05 (n=4)	15.00±0.55 (n=4)
C3H/HeNHsd	13.53±1.24 (n=4)	20.53±1.30 (n=4)	20.63±1.58 (n=4)	10.18±0.77 (n=4)	15.93±0.62 (n=4)
p-Value	0.0337	0.9237	0.0307	0.0977	0.0664
Mouse Strain	**TLR7**	**BRD1**	**BRD2**	**BRD3**	**BRD4**
C57BL/6NHsd	19.15±0.62 (n=4)	11.45±0.88 (n=4)	15.48±1.02 (n=4)	9.30±0.74 (n=4)	10.45±0.52 (n=4)
C3H/HeNHsd	21.48±1.11 (n=4)	10.30±0.76 (n=4)	13.35±0.67 (n=4)	6.30±1.01 (n=4)	9.80±0.50 (n=4)
p-Value	0.0108	0.0957	0.0132	0.0030	0.1205

Transcript levels were standardized to glycerol phosphate dehydrogenase (GPDH) levels, which were the same in the lungs of both strains. Data is summarized as mean±standard deviation for each group. For each of the 25 gene transcript levels, C57BL/6NHsd and C3H/HeNHsd were compared with the two-sided two-sample *t*-test. *p*-Values less than 0.05 were significant. As this was an exploratory study, *p*-values were not adjusted for multiple comparisons. Significant differences are shown in red.

irradiation in C57BL/6NHsd mice. Analysis of 25 representative pulmonary gene transcripts in C3H/HeNHsd mice following 20 Gy thoracic irradiation revealed an overall similar pattern to C57BL/6NHsd mice irradiated to 20 Gy to the thorax, but there were also distinct differences. In the irradiated C57BL/6NHsd mouse lung, there was an acute increase, a second interval decrease, and a clearly distinct late increase in expression of gene transcripts for *NFkβ*, *Nrf2*, *SOD2*, *TGF-β*, *SP1*, *AP1*, *TNFα*, *IL-6*, *CTGF*, and collagen 1a (Figure 2A, C and D). There was a persistent increase in expression throughout 200 days after irradiation of *vWF*, and *VEGFa* in C57BL/6NHsd mouse lungs (Figure 2B). While fibrosis-resistant C3H/HeNHsd mice also demonstrated thoracic irradiation-induced acute pulmonary increase in transcripts for *NFkβ*, *Nrf2*, *Ap1*, and *Sp1*, there was no comparable early increase in *Sod2* or collagen 1a (Figure 2C and D), and there were significantly lower levels of endothelial cell-associated gene transcripts (Figure 2B). Therefore, while pulmonary fibrosis-resistant C3H/HeNHsd mice exhibited some gene transcript elevations in common with similarly 20 Gy thoracic-irradiated C57BL/6NHsd

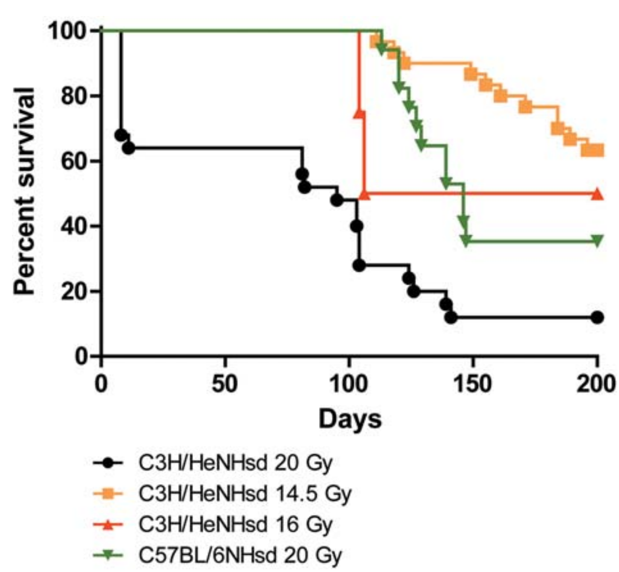

Figure 1. *In vivo survival of thoracic irradiated C3H/HeNHsd and C57BL/6NHsd mice. In vivo survival curves were generated following thoracic irradiation of groups of mice (n=20 per group).*

Table II. *Comparison of Gene Transcript Levels in 20 Gy Thoracic Irradiated C3H/HeNHsd Compared to C57BlL/6NHsd Mouse Lungs.*

	p-Value for **C57BL/6NHsd** mice calculated at day							
	2	14	28	60	100	125	150	200
vWF	Green	Green	Green	Green	Green	Green	Green	Green
TGFb	White	Green	White	Red	Red	Green	Green	Green
TNFa	Green	Green	Green	White	White	White	Green	Green
FGF1	Green	Green	White	Green	Green	Green	Green	Green
VEGFa	Green	White	Green	Green	Green	Green	Green	Green
CTGF	Green	Green	Green	Green	Green	Green	Green	Green
SOD2	Green	Green	White	White	Green	Green	Green	Green
IL6	Green	White	White	White	White	Green	Green	Green
NFkb	Green	White	White	White	White	Green	Green	Green
NFE212	Green	Green	White	Red	Red	Green	Green	Green
Sp1	Green	White	White	Red	Red	Green	Green	Green
Ap1	Green	White	White	Red	Red	Green	Green	Green
Lysl Ox	Green	Green	White	Red	White	Green	Green	Green
IGFbp7	Red	Red	White	Green	Green	Green	Green	Green
TLR4	Red	White	White	White	Green	White	Green	Green
TLR1	Green	Green	Green	Green	Green	Green	Green	Green
TLR2	Red	Red	White	Red	Red	Green	Green	Green
TLR5	Green	Green	Green	Green	Green	Green	Green	Green
TLR6	Green	Green	White	Green	White	White	Green	Green
TLR7	Green	Green	Green	White	Green	Green	Green	Green
Col1A	White	NA	Green	Green	White	White	White	Green
BRD1	Red	Red	Green	Green	Green	Green	Red	Red
BRD2	Green	Green	Green	Green	Green	Green	Green	White
BRD3	Red	Red	White	Green	Green	Green	Red	Red
BRD4	Red	Red	White	Green	Green	Green	Red	Red

	p-Value for **C3H/HeNHsd** mice calculated at day							
	2	14	28	60	100	125	150	200
vWF	White	White	Green	Green	Green	Green	Green	Green
TGFb	Green	Green	Green	Green	Green	Green	Green	Green
TNFa	Green	Green	Green	White	Green	Green	Green	Green
FGF1	White	White	Red	Red	Red	White	White	White
VEGFa	Green	Green	Green	Green	Green	Green	Green	Green
CTGF	Green	Green	Green	Green	Green	Green	Green	Green
SOD2	White	White	Green	Green	Green	Green	Green	Green
IL6	Green	Green	Green	Green	Green	Green	Green	Green
NFkb	Green	Green	Green	Green	Green	Green	White	Green
NFE212	White	Green	Green	Green	Green	Green	Green	Green
Sp1	White	Green	Green	Green	White	Green	Green	Green
Ap1	Green	Green	Red	Red	Red	Green	Green	Green
Lysl Ox	Green	Green	Green	Green	Green	Green	Green	Green
IGFbp7	Red	White	Red	Red	White	White	White	White
TLR4	Red	Red	Red	Red	White	White	White	White
TLR1	Green	Green	Green	Green	Green	Green	Green	Green
TLR2	White	Red	White	Red	Red	Green	Green	Green
TLR5	Green	Green	Green	Green	Green	Green	Green	Green
TLR6	Green	Green	Green	Green	Green	Green	Green	Green
TLR7	Green	Green	Green	White	Green	Green	Green	Green
Col1A	Green	White	White	White	White	White	White	White
BRD1	Green	Green	Green	Green	Green	Green	Green	Green
BRD2	Green	Green	Green	Green	Green	Green	Green	Green
BRD3	Green	Green	Green	Green	Green	Green	Green	Green
BRD4	Green	Green	Green	Green	Green	Green	Green	Green

The left table is for C57BL/6NHsd and the right table is for C3H/HeNHsd mouse lungs. A green cell color indicates that the level of that gene transcript at the corresponding day is significantly higher than day 0. A red cell color indicates that the level of that gene transcript at the corresponding date is significantly lower than day 0. A white cell color indicates that the level of that gene transcript at the corresponding date is not significantly different from day 0. Results are based on the p-values for comparisons between each day 0.

mice; the time course of elevation of several transcripts including *Sod2, Tgfb,* collagen 1a, *Vwf*, and *Vegf* differed. C3H/HeNHsd mice irradiated to lower doses of 14.5 Gy or 16 Gy showed the same temporal pattern of gene expression as did the 20-Gy irradiated mice (data not shown).

Distinct expression patterns of Tlr4 transcripts in the irradiated lungs of C57BL/6NHsd compared to C3H/HeNHsd mice. Levels of expression of Tlr family receptor RNA transcripts were measured in irradiated lungs of each mouse strain. In C57BL/6NHsd mouse lung, there was an acute phase and latent period decrease, followed by late increase at the time of detectable pulmonary fibrosis in transcripts for *Tlr4* (Figure 2E) and *Igfbp7* (Figure 2C). A prominent difference was the elevated levels of *Tlr4* in C57BL/6NHsd mouse lungs during the late fibrotic phase, which was absent in lungs of C3H/HeNHsd mice (Figure 2E).

Reciprocal patterns of elevated bromodomain epigenetic reader protein gene transcripts in C3H/HeNHsd compared to C57BL/6NHsd mouse lung. A major difference between mouse strains following 20 Gy thoracic irradiation was

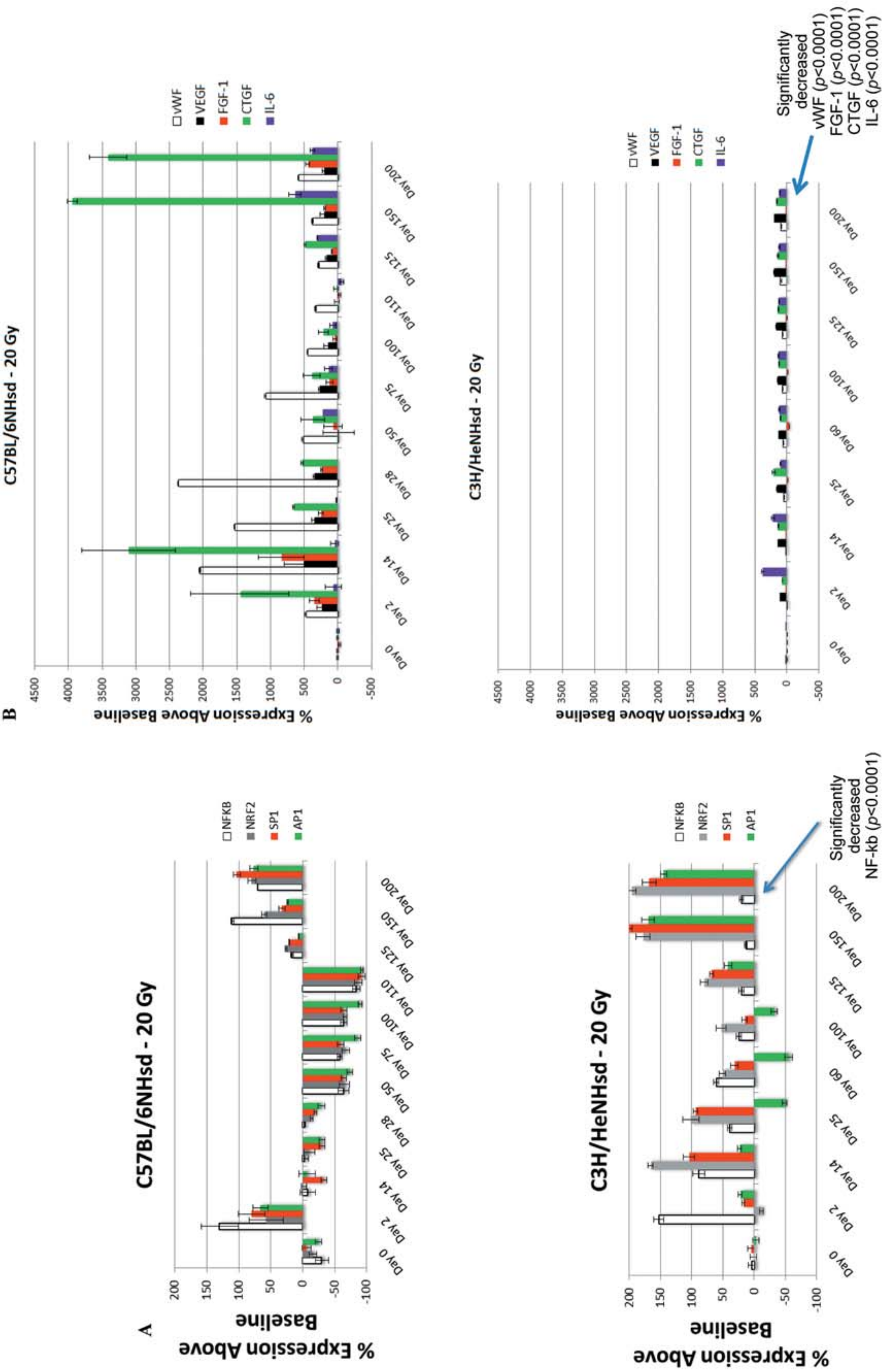

Figure 2. *Continued*

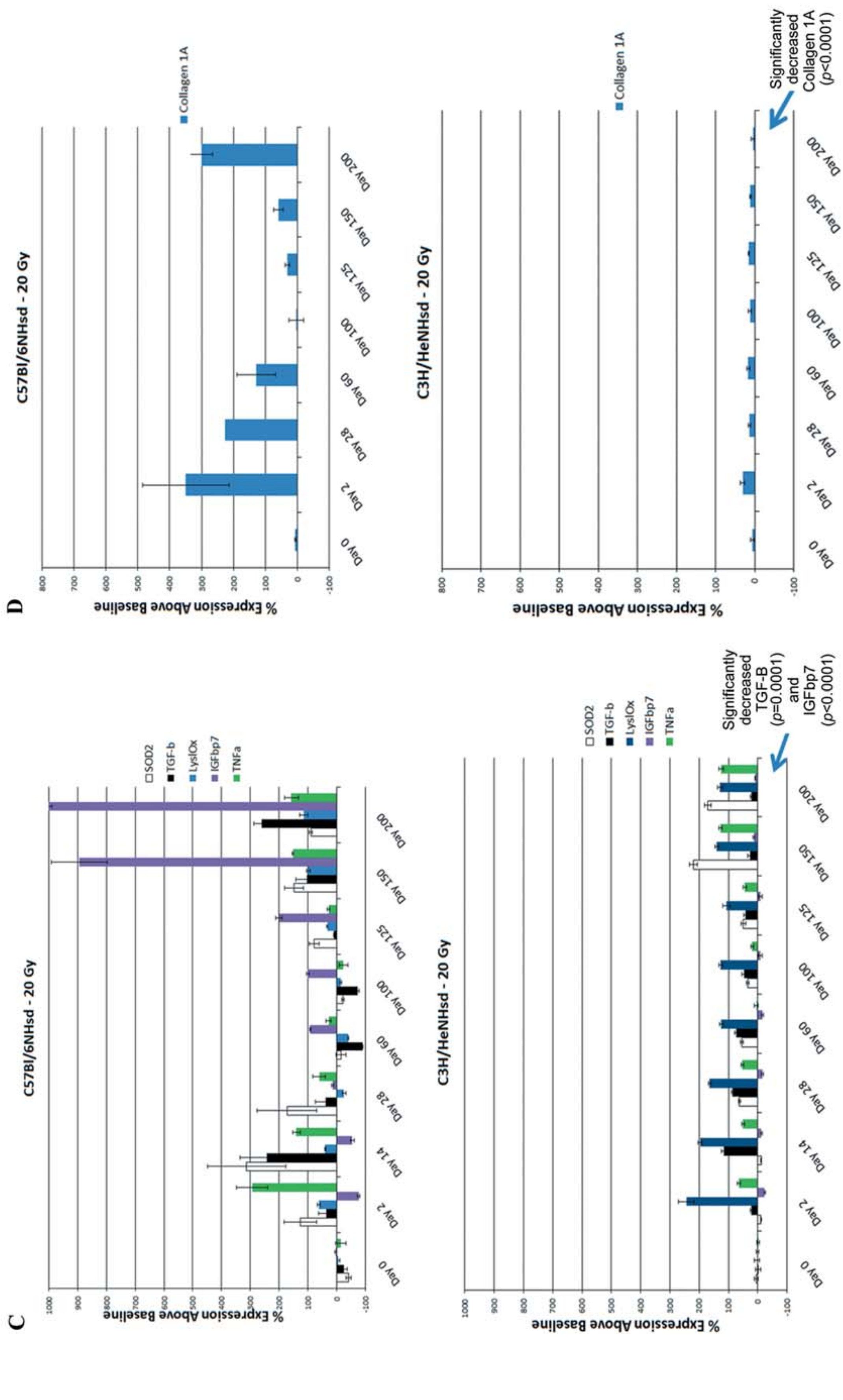

Figure 2. *Continued*

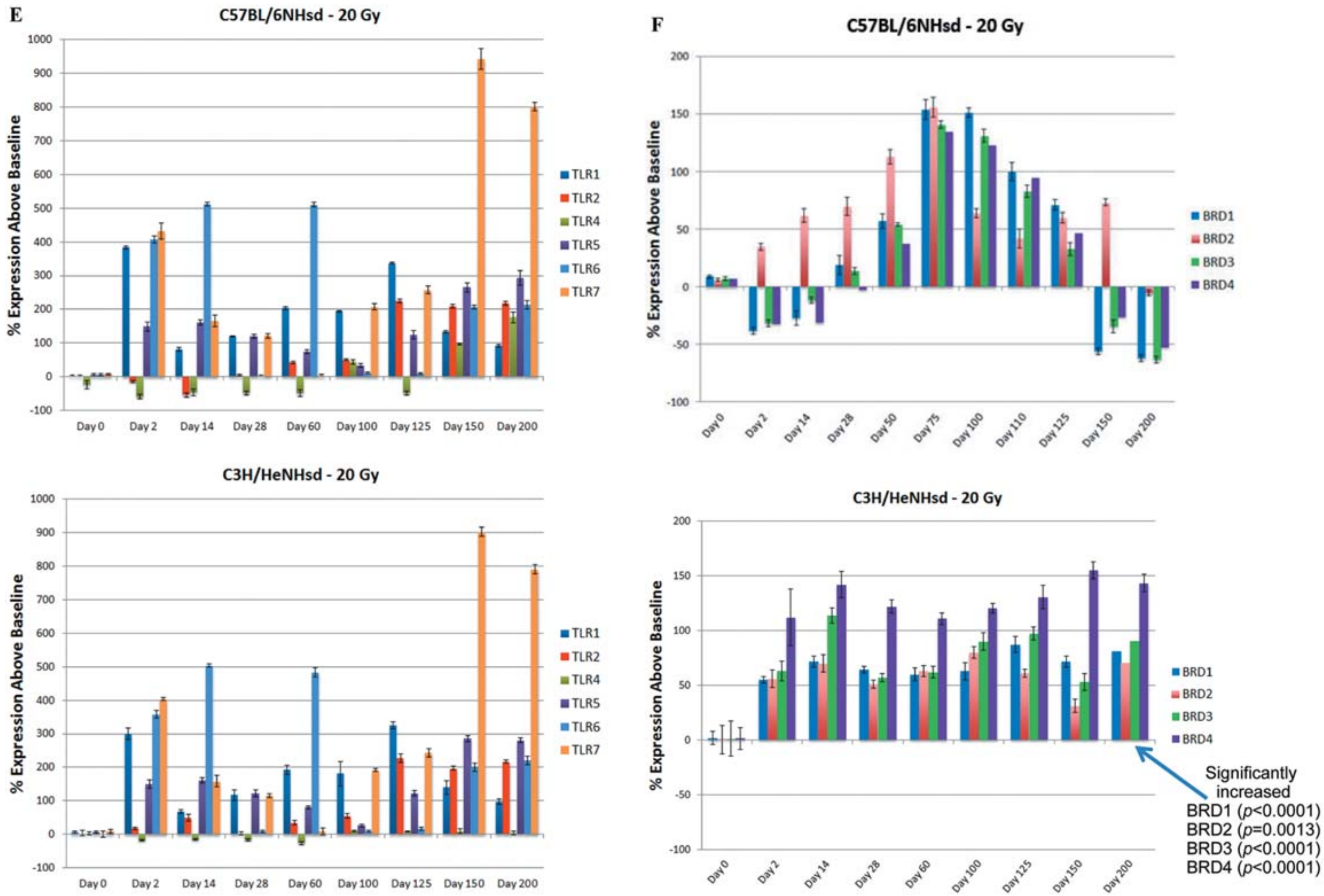

Figure 2. *Distinct patterns of irradiation induction of mRNA transcripts for acute phase, latent phase, and late fibrotic period transcript genes in lungs of C3H/HeNHsd compared to C57BL/6NHsd mice. C57BL/6NHsd and C3H/HeNHsd mice were irradiated to 20 Gy to the thoracic cavity. The mice were sacrificed at serial time points after irradiation, lungs removed, immediately frozen on dry ice, mRNA extracted, and real time RT-PCR was performed using primers specific for promoters associated with each of multiple genes. Baseline levels of each gene transcript relative to control GDPH RNA are shown in Table 1. Each panel shows relative levels over 200 days after thoracic irradiation standardized to the baseline level for that mouse strain as shown in Table I. A: pulmonary early response genes, nuclear factor kappa-light-chain-enhancer of activated B cells (Nfkb) , nuclear factor (erlythroid-derived 2)-like 2 (Nrf2), transcription factor Sp1 (Sp-1), activator protein 1 (Ap-1); B: endothelial cell markers, von Willebrand factor (Vwf) , vascular endothelial growth factor (Vegf), fibroblast growth factor-1 (Fgf1) connective tissue growth factor (Ctgf), IL-6; C: genes associated with onset of pulmonary fibrosis, manganese superoxide dismutase (Sod2) , transfroming growth factor beta (Tgfb), lysyl oxidase (Lox), insulin-like growth factor bp7 (Igfbp7), tumor necrosis factor alpha (Tnfa) ; D: collagen1a ; E: toll-like receptors, Tlr1, Tlr2, Tlr4, Tlr5, Tlr6, Tlr7; and F: bromodomain epigenetic reader proteins, Brd1, Brd2, Brd3, Brd4 . The pattern of post-irradiation data is shown in Table II and quantitation of data is shown in Tables III-IV. (A-D top panels reproduced from Kalash R, Epperly MW, Goff J, Dixon T, Sprachman MM, Zhang X, Shields D, Cao S, Franicola D, Wipf P, Berhane H, Wang H, Au J, Greenberger JS: Amelioration of irradiation pulmonary fibrosis by a water-soluble bi-functional Sulfoxide radiation mitigator (MMS350). Radiat Res 180(5): 474-490, 2013with permission of the publisher).*

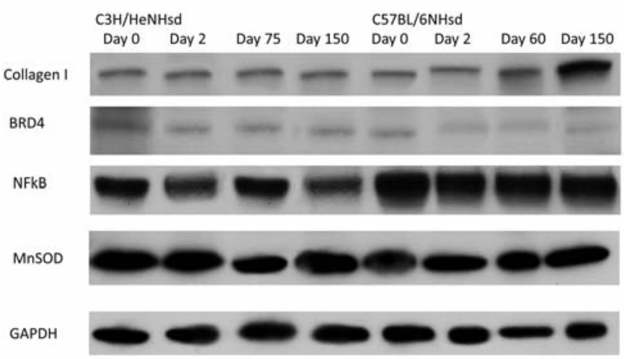

Figure 3. *Irradiation-induced proteins in lungs of 20 Gy-irradiated C57BL/6NHsd compared with C3H/HeNHsd mice. To correlate levels of SOD2, NFkβ, collagen 1a, and Brd4 RNA transcripts with protein in post irradiation lungs, tissue was removed from groups of five C3H/HeNHsd and C57BL/6NHsd female mice irradiated to 20Gy to the thoracic cavity at day 2, day 75, and day 150. Western blot analysis was then performed using antibodies, and analyzed for band densities as described in the methods and in (24). Quantitative analysis of densitometry is in Supplemental Table III.*

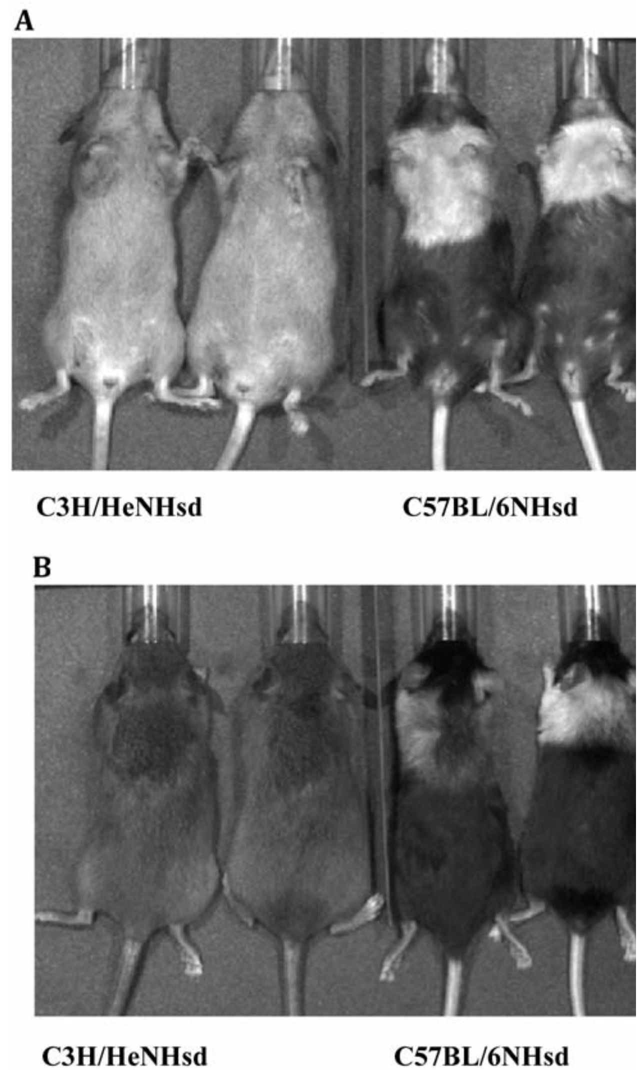

Figure 4. *C3H/HeNHsd mice display less coat color change than C57BL/6NHsd mice following 20 Gy thoracic radiation. C57BL/6NHsd and C3H/HeNHsd female mice were irradiated to 20 Gy to the thoracic cavity. The IVIS imaging system was used to take ventral (A) and dorsal (B) images at 47 days post irradiation for evaluation of coat changes.*

observed with pulmonary levels of transcripts for bromodomain epigenetic reader proteins (*Brd1-4*). In C57BL/6NHsd mouse lungs, there were initial low levels of *Brd1*, -3 and -4, then increases during the latent period (days 50-125) in expression of *Brd1-4*, followed by clear decreases at day 150 when pulmonary fibrosis was detected (Figure 2F), while levels of *Brd2* rose earlier at day 2 and persisted to day 50, levels were also low at day 200 in C57BL/6NHsd mouse lungs (Table II). In contrast, C3H/HeNHsd mouse lung showed increased expression of transcripts for *Brd1-4* during the acute phase that persisted over 200 days (Figure 2F). Thus, the irradiated C57BL/6NHsd mouse lung showed a distinct pattern of late decrease in levels of *Brd1-4* transcripts beginning with the onset of fibrosis (Figure 2F). While pre-irradiation pulmonary levels of *Brd2* and *Brd3* were elevated in C57BL/6NHsd mice, there were no significant differences in levels of *Brd1* or *Brd4* between strains (Table I). A summary of the comparative differences between the mouse strains in all 25 pulmonary gene transcript levels over time after lung irradiation is shown in Table II and statistical analysis in Tables III-IV.

Pulmonary protein levels are concordant with gene transcript levels in thoracic-irradiated C3H/HeNHsd and C57BL/ 6NHsd mice. We next determined whether increased gene transcript levels correlated with increased levels of protein. Representative proteins tested included two that have been associated with the acute pulmonary radiation reaction between days 1 and 14, a promoter-binding protein associated with the oxidative stress response (NFkβ), a radiation-protective antioxidant enzyme, MnSOD, and a protein associated with pulmonary fibrosis (collagen 1A). We also measured levels of Brd4 protein. Each protein was compared at times that corresponded to transcript levels in irradiated C57BL/6NHsd compared to C3H/HeNHsd mouse lungs (Figure 3) (Table V). In some cases, elevated RNA transcript levels were not concordant with elevated protein levels (NF-kβ, MnSOD) at the times tested, but in other cases, there was concordance. In C3H/HeNHsd mouse lung tissue at day 150, collagen 1a protein (elevated in pulmonary fibrosis) was significantly lower than levels in lungs of irradiated C57BL/6NHsd mice, while Brd4 protein level was significantly higher than the levels in C57BL/6NHsd mouse

Table III. *Gene expression in lungs of 20-Gy irradiated C57BL/6NHsd mice.*

Day	*vWF*	*TGFb*	*TNFa*	*FGF1*	*VEGFa*
0	–0.33±39.07 (n=6)	–25.60±26.54 (n=5)	–14.00±45.74 (n=6)	–28.17±41.02 (n=6)	–5.80±43.60 (n=5)
2	656.60±284.71 (n=5)	35.60±59.34 (n=5)	293.46±121.95 (n=5)	329.71±218.05 (n=7)	211.60±127.47 (n=5)
	p=0.0003	p=0.0684	p=0.0003	p=0.0023	p=0.0069
14	2881.17±2323.88 (n=6)	243.00±187.15 (n=4)	139.83±26.14 (n=4)	1205.20±791.34 (n=5)	1009.57±1216.80 (n=7)
	p=0.0125	p=0.0145	p=0.0003	p=0.0039	p=0.0958
28	2366.29±2279.84 (n=7)	37.88±100.57 (n=8)	61.00±48.97 (n=5)	61.34±161.85 (n=5)	341.25±169.37 (n=4)
	p=0.0282	p=0.2007	p=0.0276	p=0.2200	p=0.0029
60	519.67±55.43 (n=3)	–90.78±3.90 (n=5)	28.20±17.30 (n=4)	73.33±83.58 (n=3)	91.00±28.90 (n=4)
	p<0.0001	p=0.0006	p=0.1209	p=0.0388	p=0.0067
100	449.43±86.67 (n=7)	–73.60±12.60 (n=5)	–23.80±34.52 (n=5)	44.60±24.10 (n=5)	179.33±82.98 (n=6)
	p<0.0001	p=0.0065	p=0.7031	p=0.0069	p=0.0015
125	387.20±198.74 (n=5)	10.40±3.51 (n=5)	27.90±10.98 (n=5)	84.60±15.57 (n=5)	167.60±133.55 (n=5)
	p=0.0011	p=0.0169	p=0.0785	p=0.0003	p=0.0247
150	378.67±30.66 (n=3)	104.20±81.28 (n=5)	152.33±4.04 (n=3)	196.33±52.17 (n=3)	199.33±34.82 (n=3)
	p<0.0001	p=0.0094	p=0.0005	p=0.0002	p=0.0005
200	584.50±26.84 (n=4)	259.75±53.65 (n=4)	157.83±58.40 (n=6)	447.00±72.17 (n=4)	207.50±25.15 (n=4)
	p<0.0001	p<0.0001	p=0.0002	p<0.0001	p=0.0001
Day	***CTGF***	***SOD2***	***IL6***	***NFkb***	***NFE212***
0	3.50±28.01 (n=6)	–41.50±20.15 (n=6)	–1.75±29.55 (n=4)	62.40±27.13 (n=5)	–25.83±15.41 (n=6)
2	1724.40±1855.84 (n=5)	126.67±137.59 (n=6)	150.50±37.56 (n=4)	176.33±40.06 (n=6)	78.83±95.51 (n=6)
	p=0.0473	p=0.0142	p=0.0007	p=0.0004	p=0.0243
14	3104.67±1209.43 (n=3)	313.50±333.58 (n=6)	–9.87±38.81 (n=3)	101.83±40.79 (n=6)	2.33±10.80 (n=6)
	p=0.0003	p=0.0264	p=0.7643	p=0.0988	p=0.0043
28	421.00±451.75 (n=5)	172.84±292.60 (n=8)	18.70±5.05 (n=4)	96.67±31.03 (n=6)	–25.00±22.66 (n=6)
	p=0.0483	p=0.1016	p=0.2214	p=0.0860	p=0.9421
60	373.67±211.11 (n=3)	–15.83±43.23 (n=6)	–9.00±38.97 (n=4)	34.45±13.00 (n=6)	–64.55±21.04 (n=6)
	p=0.0027	p=0.2168	p=0.7768	p=0.0511	p=0.0046
100	248.00±68.71 (n=4)	–21.00±10.88 (n=7)	88.20±110.49 (n=5)	40.86±24.42 (n=7)	–67.14±17.58 (n=7)
	p<0.0001	p=0.0395	p=0.1618	p=0.1803	p=0.0010
125	489.00±166.78 (n=5)	77.80±38.28 (n=5)	302.40±199.68 (n=5)	117.33±4.73 (n=3)	26.00±6.24 (n=3)
	p=0.0001	p=0.0001	p=0.0205	p=0.0150	p=0.0010
150	3944.67±478.16 (n=3)	148.33±55.90 (n=3)	638.33±62.07 (n=3)	210.00±1.00 (n=3)	59.67±11.50 (n=3)
	p<0.0001	p=0.0001	p<0.0001	p=0.0001	p=0.0001
200	3416.25±135.91 (n=4)	90.00±11.40 (n=4)	379.75±25.91 (n=4)	170.25±11.76 (n=4)	79.25±7.93 (n=4)
	p<0.0001	p<0.0001	p<0.0001	p=0.0002	p<0.0001
Day	***Sp1***	***Ap1***	***Lysl Ox***	***IGFbp7***	***TLR4***
0	–12.00±22.93 (n=7)	–18.00±15.06 (n=6)	–5.40±13.70 (n=5)	3.00±5.00 (n=3)	–23.00±25.65 (n=4)
2	111.50±26.88 (n=6)	77.83±20.43 (n=6)	62.00±8.89 (n=3)	–76.33±6.03 (n=3)	–59.00±12.91 (n=4)
	p<0.0001	p<0.0001	p=0.0003	p=0.0001	p=0.0461
14	–20.08±15.13 (n=6)	–14.86±35.14 (n=7)	39.67±4.51 (n=3)	–54.33±11.15 (n=3)	–45.75±19.12 (n=4)
	p=0.4778	p=0.8430	p=0.0017	p=0.0012	p=0.2048
28	–28.17±9.87 (n=6)	–31.00±15.85 (n=7)	–25.67±11.68 (n=3)	13.70±6.02 (n=3)	–48.67±9.61 (n=3)
	p=0.1386	p=0.1598	p=0.0778	p=0.0770	p=0.1667
60	–59.82±18.71 (n=6)	–79.15±10.25 (n=6)	–39.33±2.08 (n=3)	91.67±3.06 (n=3)	–49.50±20.44 (n=4)
	p=0.0019	p<0.0001	p=0.0062	p<0.0001	p=0.1572
100	–67.14±24.67 (n=7)	–90.54±6.92 (n=7)	–13.67±6.03 (n=3)	101.00±7.55 (n=3)	44.40±15.44 (n=5)
	p=0.0010	p<0.0001	p=0.3713	p<0.0001	p=0.0017
125	20.80±11.14 (n=5)	6.60±2.30 (n=5)	32.67±3.51 (n=3)	199.67±18.88 (n=3)	–48.40±12.82 (n=5)
	p=0.0150	p=0.0059	p=0.0038	p=0.0001	p=0.0918
150	32.00±8.89 (n=3)	24.00±11.14 (n=3)	98.33±10.07 (n=3)	893.67±167.82 (n=3)	96.80±5.26 (n=5)
	p=0.0140	p=0.0039	p<0.0001	p=0.0008	p<0.0001
200	103.00±14.31 (n=4)	76.25±17.80 (n=4)	114.33±25.70 (n=3)	1029.33±70.12 (n=3)	176.17±40.26 (n=6)
	p<0.0001	p<0.0001	p=0.0001	p<0.0001	p<0.0001

Table III. *Continued*

Table III. *Continued*

Day	*TLR1*	*TLR2*	*TLR5*	*TLR6*	*TLR7*
0	2.33±4.93 (n=3)	2.80±2.55 (n=3)	5.20±9.00 (n=3)	6.00±5.29 (n=3)	8.30±4.03 (n=3)
2	384.00±58.41 (n=3) *p*=0.0004	–14.00±5.00 (n=3) *p*=0.0066	148.67±25.11 (n=3) *p*=0.0007	407.33±17.79 (n=3) *p*<0.0001	432.33±40.92 (n=3) *p*=0.0001
14	82.00±10.82 (n=3) *p*=0.0003	–53.33±12.01 (n=3) *p*=0.0014	161.67±13.20 (n=3) *p*=0.0001	511.67±9.71 (n=3) *p*<0.0001	166.00±30.27 (n=3) *p*=0.0009
28	121.00±11.53 (n=3) *p*=0.0001	5.33±4.04 (n=3) *p*=0.4106	120.67±10.02 (n=3) *p*=0.0001	2.93±3.58 (n=3) *p*=0.4525	122.00±12.00 (n=3) *p*=0.0001
60	203.67±8.08 (n=3) *p*<0.0001	–42.33±6.81 (n=3) *p*=0.0004	74.67±11.68 (n=3) *p*=0.0012	511.00±11.53 (n=3) *p*<0.0001	4.67±6.11 (n=3) *p*=0.4385
100	194.33±13.32 (n=3) *p*<0.0001	–51.00±4.58 (n=3) *p*=0.0001	33.33±10.50 (n=3) *p*=0.0244	12.33±4.51 (n=3) *p*=0.1897	208.00±15.13 (n=3) *p*<0.0001
125	337.67±32.81 (n=3) *p*=0.0001	225.00±11.00 (n=3) *p*<0.0001	124.00±21.93 (n=3) *p*=0.0010	9.53±5.28 (n=3) *p*=0.4591	257.67±18.50 (n=3) *p*<0.0001
150	134.00±14.42 (n=3) *p*=0.0001	209.33±10.69 (n=3) *p*<0.0001	265.00±24.58 (n=3) *p*=0.0001	206.33±9.71 (n=3) *p*<0.0001	942.33±52.20 (n=3) *p*<0.0001
200	91.67±6.66 (n=3) *p*<0.0001	217.67±10.02 (n=3) *p*<0.0001	294.00±37.51 (n=3) *p*=0.0002	213.67±22.68 (n=3) *p*=0.0001	801.33±22.05 (n=3) *p*<0.0001

Day	*Col1A*	*BRD1*	*BRD2*	*BRD3*	*BRD4*
0	6.50±4.19 (n=4)	8.80±3.70 (n=5)	6.28±3.21 (n=5)	7.00±3.39 (n=5)	7.20±3.35 (n=5)
2	349.00±233.42 (n=3) *p*=0.0289	–37.82±6.11 (n=5) *p*<0.0001	34.98±6.66 (n=5) *p*<0.0001	–31.60±7.13 (n=5) *p*<0.0001	–31.80±8.47 (n=5) *p*<0.0001
14	– (n=0)	–26.66±4.63 (n=5) *p*<0.0001	61.80±13.52 (n=5) *p*<0.0001	–11.60±6.19 (n=5) *p*=0.0004	–30.78±10.89 (n=5) *p*=0.0001
28	225.50±85.56 (n=2) *p*=0.0042	19.40±6.80 (n=5) *p*=0.0156	69.92±19.41 (n=5) *p*=0.0001	13.80±7.19 (n=5) *p*=0.0922	–2.44±12.92 (n=5) *p*=0.1449
60	128.50±45.21 (n=4) *p*=0.0017	57.08±9.94 (n=5) *p*<0.0001	112.80±9.12 (n=5) *p*<0.0001	54.20±12.52 (n=5) *p*<0.0001	37.40±12.01 (n=5) *p*=0.0006
100	3.58±13.89 (n=4) *p*=0.7007	151.60±5.86 (n=5) *p*<0.0001	64.00±10.22 (n=5) *p*<0.0001	131.20±12.83 (n=5) *p*<0.0001	123.20±7.66 (n=5) *p*<0.0001
125	30.50±30.16 (n=4) *p*=0.1660	70.60±9.61 (n=5) *p*<0.0001	59.80±6.30 (n=5) *p*<0.0001	33.00±6.20 (n=5) *p*<0.0001	47.02±8.16 (n=5) *p*<0.0001
150	58.50±69.36 (n=4) *p*=0.1851	–55.82±8.51 (n=5) *p*<0.0001	73.40±6.69 (n=5) *p*<0.0001	–34.20±11.54 (n=5) *p*=0.0001	–25.80±7.36 (n=5) *p*<0.0001
200	299.33±34.27 (n=3) *p*<0.0001	–61.60±3.05 (n=5) *p*<0.0001	–4.80±22.69 (n=5) *p*=0.3111	–63.20±5.72 (n=5) *p*<0.0001	–52.20±9.26 (n=5) *p*<0.0001

Data summary using mean±SD and group comparisons, where *p* is the *p*-value for the comparison of gene expression in lungs of C57BL/6NHsd mice between each day and day 0 for the corresponding gene, using the two-sided two-sample *t*-test.

lung (Figure 3) (Table V). The data for collagen 1a and Brd4 were concordant with RNA transcript levels at day 150 (Figure 2D and F, respectively).

Distinct lung histopathology in thoracic-irradiated C3H/HeNHsd compared to C57BL/6NHsd mice. C3H/HeNHsd mice showed no physical evidence of late coat greying (Figure 4) and no histopathological evidence of pulmonary fibrosis after any of the three radiation doses, and dying mice showed no detectable pulmonary fibrosis (Figure 5A-D). By 150 days post-irradiation, C57BL/6NHsd mice displayed pulmonary organizing alveolitis (fibrosis) (Figure 5E). These results confirm and extend those in a prior publication (24).

The histopathology of C57BL/6NHsd lung tissue showed an acute inflammatory reaction, a stable latent period, followed by a late fibrosis phase 150 days post-irradiation. In contrast, lung tissue from C3H/HeNHsd mice irradiated with 20 Gy showed a robust acute inflammatory reaction following thoracic irradiation, but no late-phase (day 150) fibrosis reaction (Figure 5D).

At acute, latent period, and late time points, (days 2, 100, and 150 post-irradiation), C57BL/6NHsd mice lungs were quantitated for fibrosis, collagen deposition, and inflammatory cell accumulation in the lungs, and results were compared against those of C3H/HeNHsd mice irradiated to 14.5,16, or 20 Gy. Light microscopic

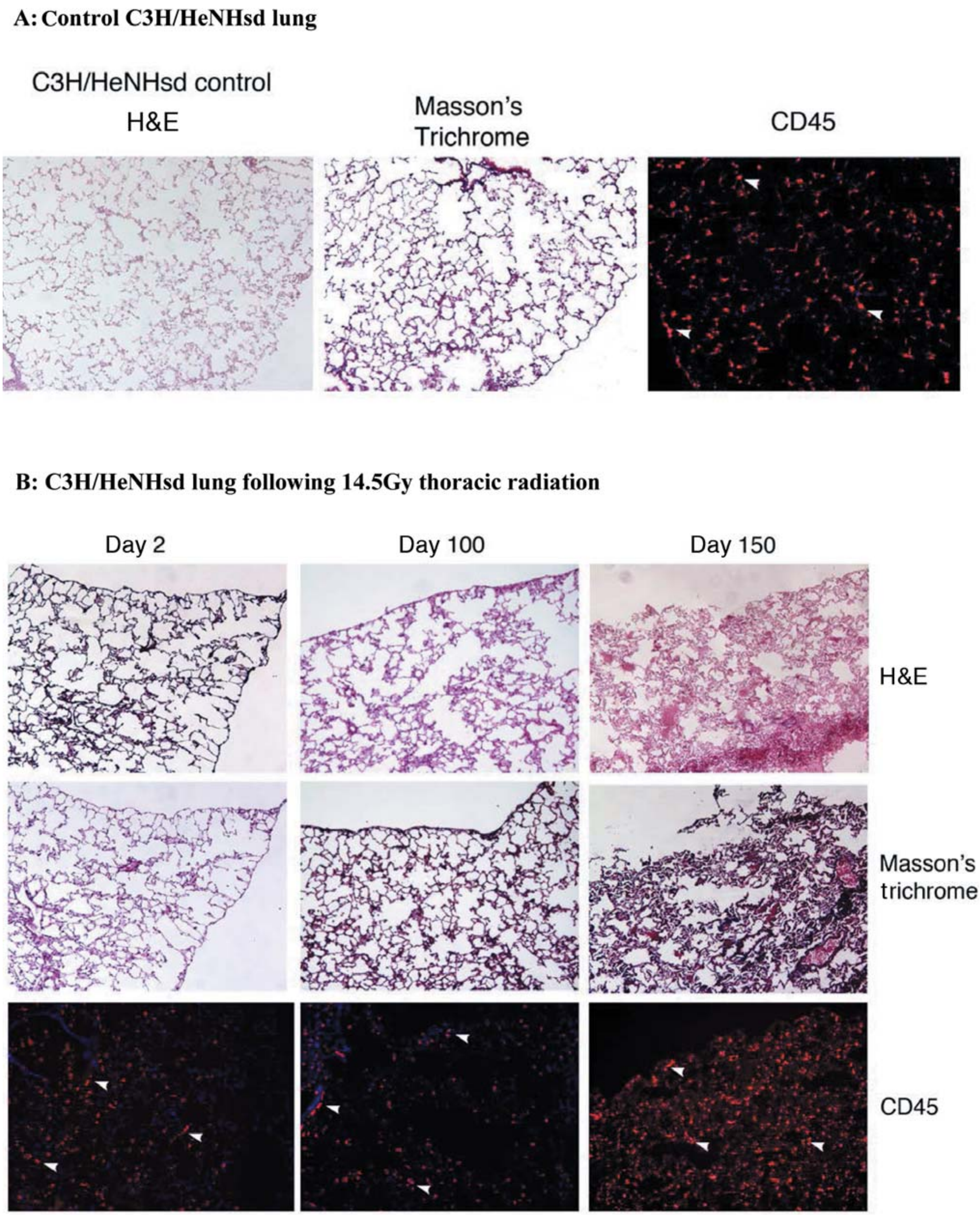

Figure 5. *Continued*

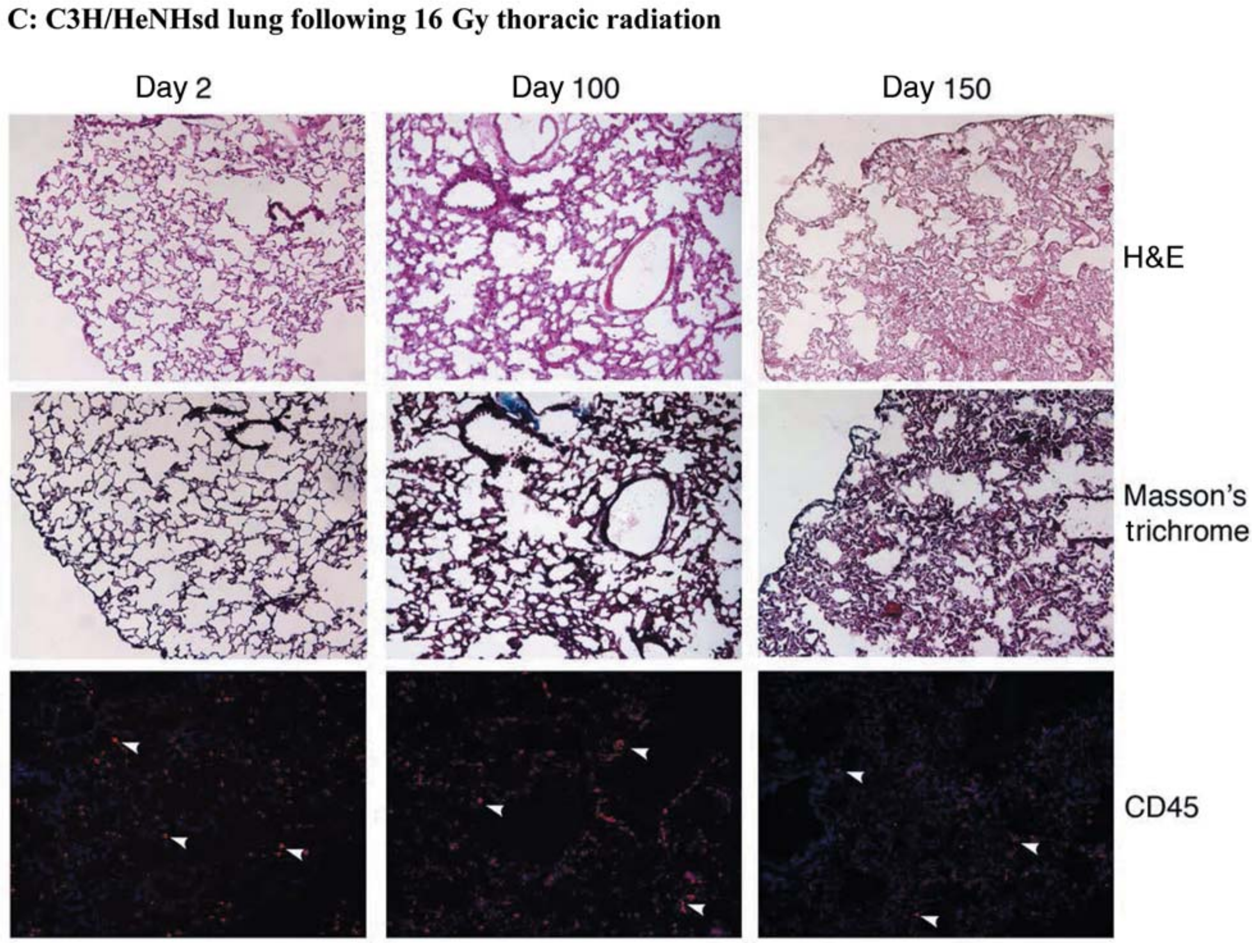

Figure 5. *Continued*

quantitation of inflammation and percentage fibrosis in H&E-stained lung sections from the acute-phase, latent period, and late-fibrotic time points was performed. As shown in Figure 5, there was a pulmonary inflammatory infiltrate during the acute phase in lungs of C57BL/6NHsd mice irradiated with 20 Gy, and an inflammatory infiltrate in the acute phase in lungs of C3H/HeNHsd mice after doses of 14.5, 16, and 20 Gy. At day 100, the lungs of C3H/HeNHsd and C57BL/6NHsd mice showed little histopathological change. Histopathological sections of lung from C57BL/6NHsd but not C3H/HeNHsd mice showed significant fibrosis at day 150 (Figure 5E).

Lack of detectable bone marrow stromal cell homing to the lungs of thoracic-irradiated C3H/HeNHsd mice. C57BL/6NHsd mice chimeric for luc+ bone marrow have been reported to display fibrosis at 150-200 days after 20 Gy thoracic irradiation, and coincident homing of luc+ bone marrow stromal cells to the lungs (24).

To determine whether luc+ marrow stromal cell homing occurred in C3H/HeNHsd mice in the absence of a detectable pulmonary fibrosis, mice were injected intraperitoneally with 1×10^6 luc+ bone marrow stromal cells prepared from C3H/HeNHsd mouse marrow according to published methods (24) using luciferase mouse gene transduced stromal cell lines derived from long term bone marrow cultures. Mice were injected at serial times for live imaging of lung migration of luc+ cells using published methods (24). At each of the three time points after 20-Gy thoracic irradiation: immediately, 67 days, or 134 days post- thoracic irradiation, C3H/HeNHsd demonstrated no detectable luc+ bone marrow stromal cell homing to the lungs (Figure 6A-D). In contrast, C57BL/6NHsd mice injected *i.p.* at day 129 after 20 Gy thoracic irradiation showed significant homing of luc+ stromal cells derived from luciferase gene-transduced cells harvested from C57BL/6NHsd long-term marrow cultures (Figure 6E). The present results with C57BL/6NHsd mice confirm and extend other results from prior studies (24).

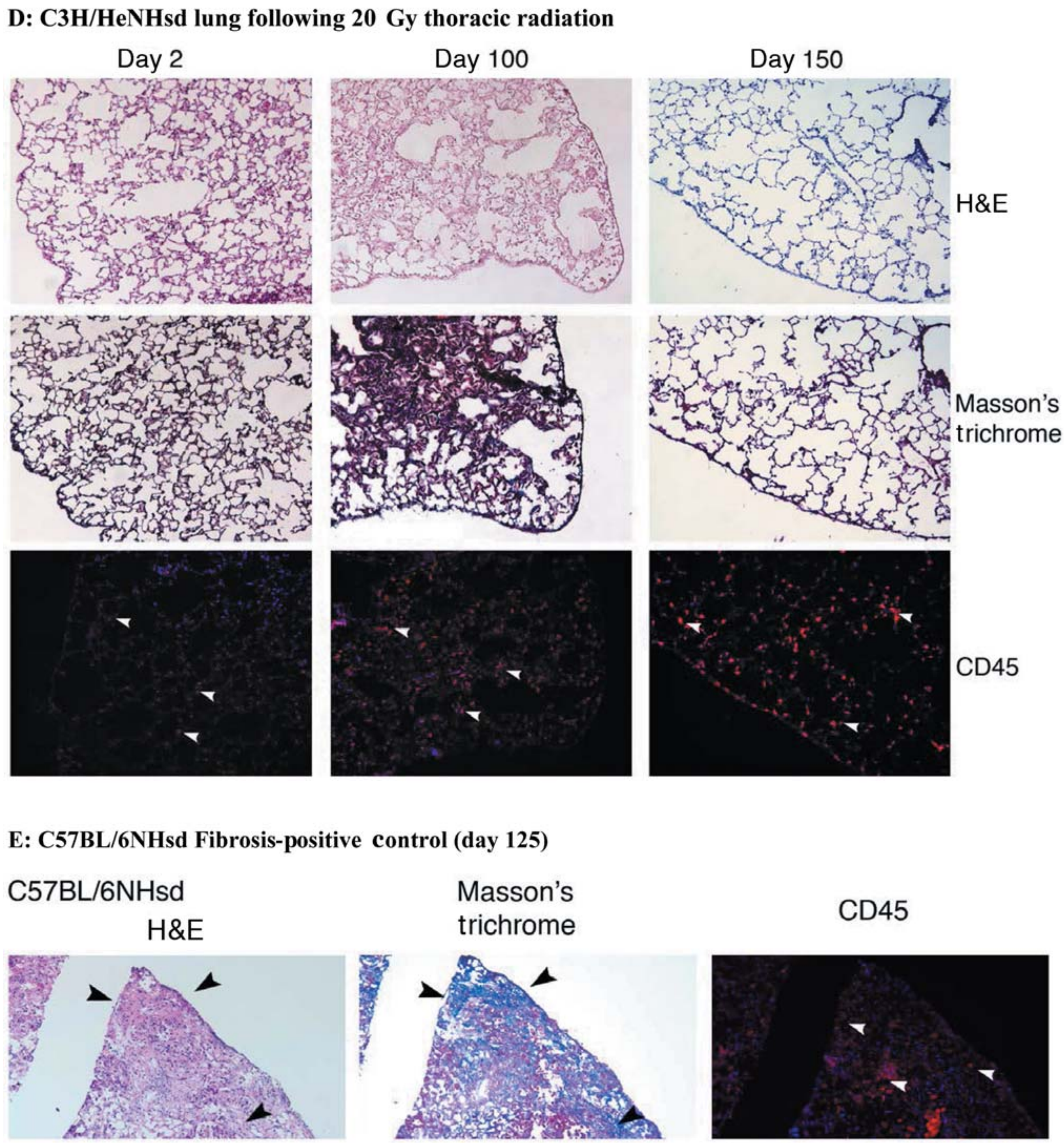

Figure 5. *Absence of pulmonary fibrosis in lungs of thoracic irradiated C3H/HeNHsd mice. Frozen sections removed at day 2, 100, or 150 from lungs of: unirradiated C3H/HeNHsd control mice (A); C3H/HeNHsd mice thoracic-irradiated to 14.5 Gy (B), 16 Gy (C), or 20 Gy (D), or C57BL/6NHsd mice thoracic-irradiated to 20 Gy (E) were stained with hematoxylin and eosin, Masson's trichrome (for collagen) or immunostained for CD45 at serial times after irradiation. Sections were collected from C3H/HeNHsd mouse lungs at day 2 (acute phase), day 100 (latent period) and day 150 (late phase). No detectable fibrosis or increased collagen was observed in control unirradiated, acute, latent or late phase lung tissue from C3H/HeNHsd mice after any irradiation dose. C57BL/6NHsd mice showed late-phase fibrosis at day 150 (E). Increased collagen (black arrows) in Masson's trichrome-stained sections (E) and increased numbers of red stained CD45+ inflammatory cells (white arrows) in perivascular distribution was seen in C57BL/6NHsd lungs in the late phase post-irradiation (E). Masson's trichrome staining of lungs from irradiated C3H/HeNHsd mice at all times was similar to control unirradiated lungs, indicating no detectable fibrosis. Low-level immunostaining for CD45 cells (white arrows) in C3H/HeNHsd lungs was similar in control unirradiated, and irradiated lungs at all phases. All images ×10 magnification.*

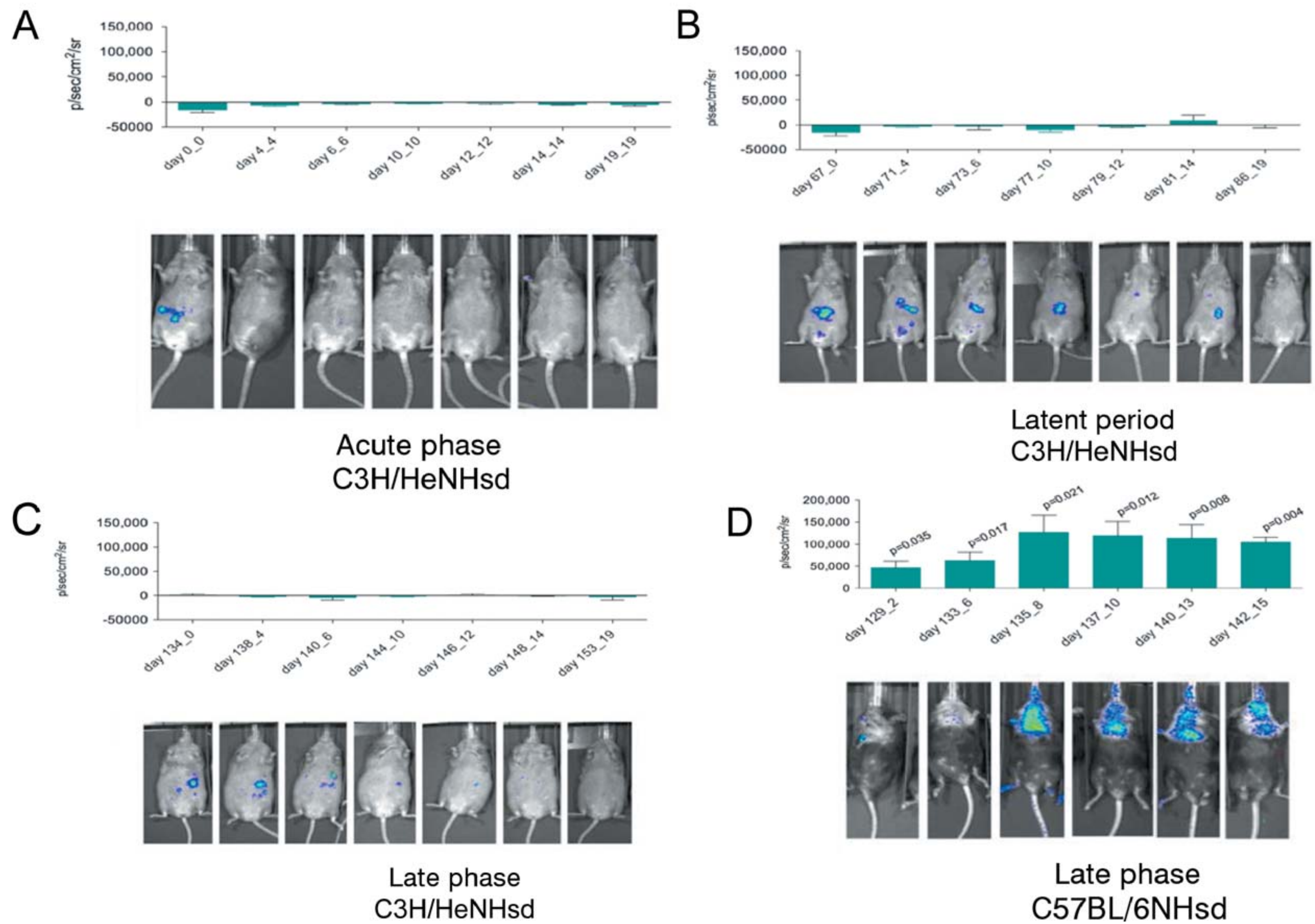

Figure 6. *Absence of detectable bone marrow stromal cell homing to the irradiated lungs of C3H/HeNHsd mice. Groups of 20 Gy thoracic-irradiated C3H/HeNHsd and C57BL/6NHsd mice were injected intraperitoneally with 1×10^6 syngeneic luc+ bone marrow stromal cells at each of four time points: immediately, at 67 days, 129 days, or 134 days post-thoracic irradiation according to published methods (28, 30). In vivo imaging revealed no detectable migration of luc+ cells to the lungs of 20 Gy thoracic-irradiated C3H/HeNHsd mice at any time point: acute phase (A), the latent period (B), or the late phase (C) . In contrast, C57BL/6NHsd mice revealed significant late phase migration of luc+ BM cells to the lungs at day 129 (D). Late-phase bioluminescence in C3H/HeNHsd mice was compared to late-phase bioluminescence in C57BL/6NHsd mouse lungs using a two-sided two-sample t-test. Pulmonary migration of luc+ cells was significantly increased ($p<0.05$) in C57BL/6NHsd compared C3H/HeNHsd mouse lungs (Figure 3D).*

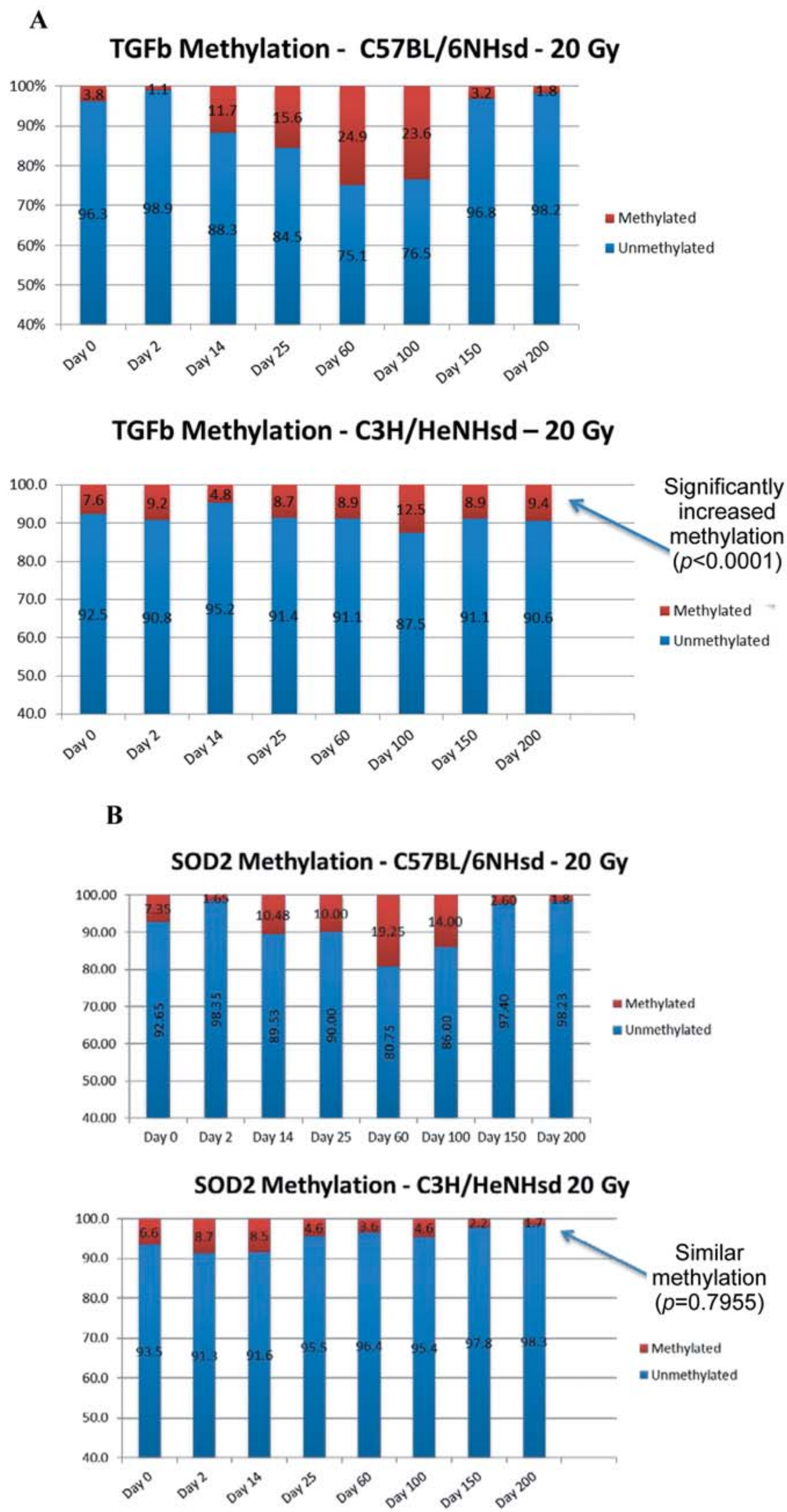

Figure 7. *Continued*

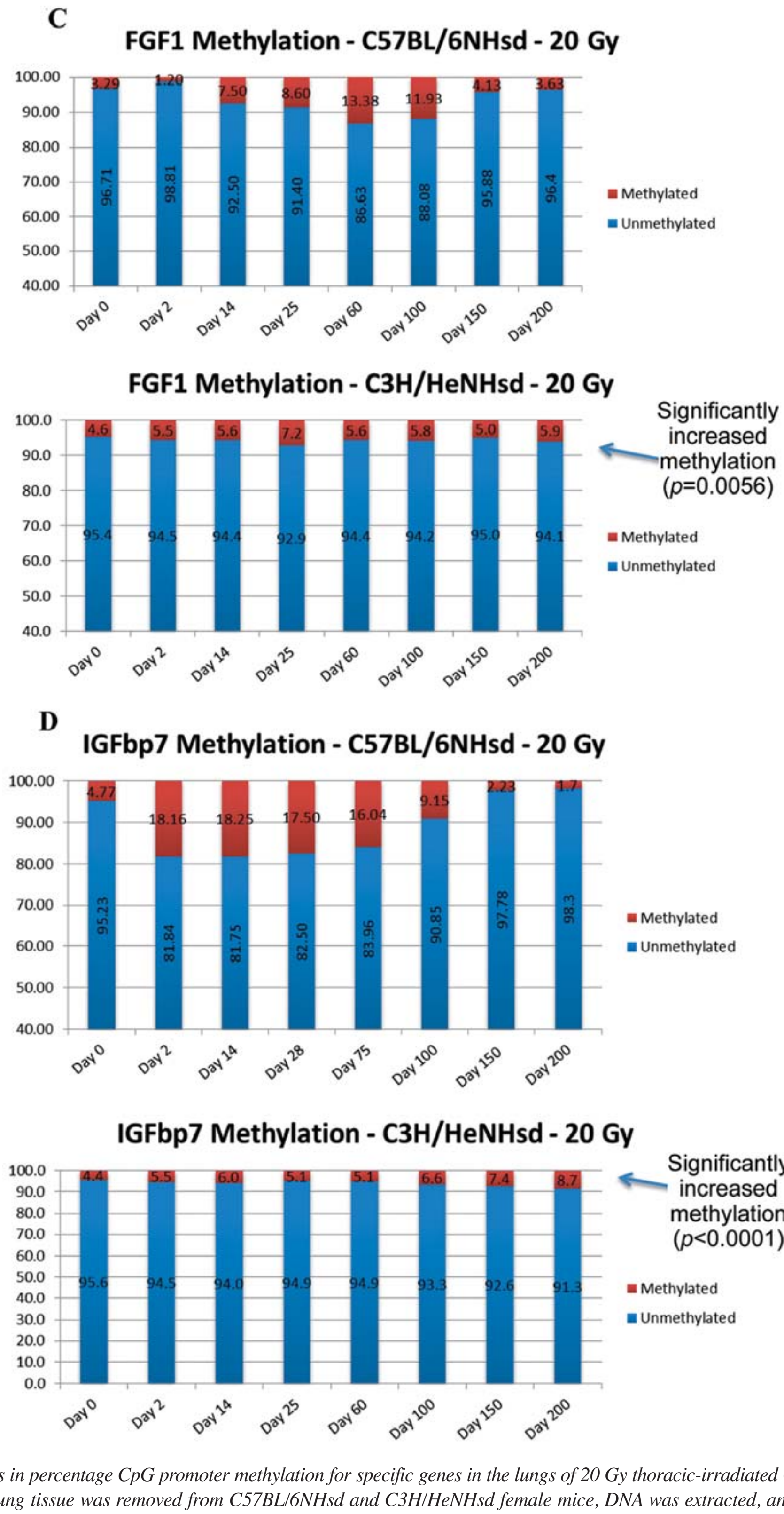

Figure 7. *Different patterns in percentage CpG promoter methylation for specific genes in the lungs of 20 Gy thoracic-irradiated C3H/HeNHsd mice compared to C57BL/6NHsd mice. Lung tissue was removed from C57BL/6NHsd and C3H/HeNHsd female mice, DNA was extracted, and CpG promoter methylation status of genes related to fibrosis was evaluated for TGF-β (A), MnSOD (B), FGF1 (C), and IGFbp7 (D). Each bar represents 100% of the promoter; the red portion represents the percentage of methylated DNA, and the blue portion represents the percentage of unmethylated DNA. There was concordance of increased methylation at respective time points where the corresponding gene transcript level was decreased. The pattern of data is shown in Table II.*

Table IV. *Gene expression in lungs of 20-Gy thoracic irradiated C3H/HeNHsd mice.*

Day	*vWF*	*TGFb*	*TNFa*	*FGF1*	*VEGFa*
0	2.13±11.08 (n=4) *p2*=0.9071	–1.25±16.34 (n=4) *p2*=0.1544	–0.75±9.91 (n=4) *p2*=0.5909	–1.25±10.12 (n=4) *p2*=0.2421	–0.50±8.76 (n=4) *p2*=0.8200
2	–0.45±9.08 (n=4) *p1*=0.7315 *p2*=0.0026	22.32±7.56 (n=4) *p1*=0.0396 *p2*=0.6742	64.73±10.73 (n=4) *p1*=0.0001 *p2*=0.0078	1.25±3.34 (n=4) *p1*=0.6555 *p2*=0.0164	100.68±13.78 (n=4) *p1*<0.0001 *p2*=0.1313
14	5.96±2.04 (n=4) *p1*=0.5214 *p2*=0.0416	116.75±12.43 (n=4) *p1*<0.0001 *p2*=0.2269	50.15±7.44 (n=4) *p1*=0.0002 *p2*=0.0006	4.13±1.47 (n=4) *p1*=0.3336 *p2*=0.0201	131.28±6.15 (n=4) *p1*<0.0001 *p2*=0.1920
28	40.00±8.69 (n=4) *p1*=0.0017 *p2*=0.0773	87.23±6.24 (n=4) *p1*=0.0001 *p2*=0.3611	52.83±8.90 (n=4) *p1*=0.0002 *p2*=0.7546	–17.33±5.07 (n=4) *p1*=0.0295 *p2*=0.3699	144.98±20.40 (n=4) *p1*<0.0001 *p2*=0.0610
60	52.95±12.79 (n=4) *p1*=0.0010 *p2*<0.0001	73.10±11.46 (n=4) *p1*=0.0003 *p2*<0.0001	4.75±13.84 (n=4) *p1*=0.5421 *p2*=0.0786	–40.10±6.69 (n=4) *p1*=0.0007 *p2*=0.0382	120.50±12.40 (n=4) *p1*<0.0001 *p2*=0.1097
100	65.25±6.24 (n=4) *p1*=0.0001 *p2*<0.0001	47.63±14.19 (n=4) *p1*=0.0040 *p2*<0.0001	19.43±8.95 (n=4) *p1*=0.0233 *p2*=0.0468	–15.75±3.77 (n=4) *p1*=0.0363 *p2*=0.0018	141.00±19.41 (n=4) *p1*<0.0001 *p2*=0.3990
125	63.50±5.20 (n=4) *p1*=0.0001 *p2*=0.0148	41.85±10.25 (n=4) *p1*=0.0042 *p2*=0.0003	44.50±9.57 (n=4) *p1*=0.0006 *p2*=0.0489	3.25±11.24 (n=4) *p1*=0.5735 *p2*=0.0001	157.50±22.49 (n=4) *p1*<0.0001 *p2*=0.8868
150	94.50±15.93 (n=4) *p1*=0.0001 *p2*<0.0001	27.25±13.57 (n=4) *p1*=0.0364 *p2*=0.1071	126.33±11.73 (n=4) *p1*<0.0001 *p2*=0.0154	5.43±6.51 (n=4) *p1*=0.3096 *p2*=0.0007	189.25±30.82 (n=4) *p1*<0.0001 *p2*=0.7012
200	88.03±5.90 (n=4) *p1*<0.0001 *p2*<0.0001	21.80±5.57 (n=4) *p1*=0.0370 *p2*=0.0001	124.00±15.12 (n=4) *p1*<0.0001 *p2*=0.2980	13.95±7.27 (n=4) *p1*=0.0505 *p2*<0.0001	193.28±10.99 (n=4) *p1*<0.0001 *p2*=0.3398

Day	*CTGF*	*SOD2*	*IL6*	*NFkb*	*NFE212*
0	–4.00±17.11 (n=4) *p2*=0.6479	5.25±14.08 (n=4) *p2*=0.0040	5.55±8.13 (n=4) *p2*=0.6506	3.50±10.21 (n=4) *p2*=0.0047	1.22±11.25 (n=4) *p2*=0.0172
2	69.75±8.15 (n=4) *p1*=0.0002 *p2*=0.1221	–11.03±1.07 (n=4) *p1*=0.0607 *p2*=0.0855	367.00±55.98 (n=4) *p1*<0.0001 *p2*=0.0007	152.88±16.54 (n=4) *p1*<0.0001 *p2*=0.3063	–12.13±6.02 (n=4) *p1*=0.0814 *p2*=0.0993
14	130.90±7.21 (n=4) *p1*<0.0001 *p2*=0.0038	–11.30±2.75 (n=4) *p1*=0.0605 *p2*=0.0928	216.75±47.06 (n=4) *p1*=0.0001 *p2*=0.0011	88.45±20.80 (n=4) *p1*=0.0003 *p2*=0.5664	165.85±6.99 (n=4) *p1*<0.0001 *p2*<0.0001
28	218.75±49.39 (n=4) *p1*=0.0001 *p2*=0.4086	63.05±6.82 (n=4) *p1*=0.0003 *p2*=0.4808	95.15±10.36 (n=4) *p1*<0.0001 *p2*<0.0001	38.63±6.44 (n=4) *p1*=0.0011 *p2*=0.0068	101.60±26.40 (n=4) *p1*=0.0004 *p2*<0.0001
60	100.73±8.46 (n=4) *p1*<0.0001 *p2*=0.0442	53.85±8.36 (n=4) *p1*=0.0010 *p2*=0.0141	117.25±17.29 (n=4) *p1*<0.0001 *p2*=0.0010	61.28±7.93 (n=4) *p1*=0.0001 *p2*=0.0064	50.90±9.65 (n=4) *p1*=0.0005 *p2*<0.0001
100	120.75±11.95 (n=4) *p1*<0.0001 *p2*=0.0107	34.95±8.08 (n=4) *p1*=0.0106 *p2*<0.0001	23.90±8.26 (n=4) *p1*<0.0001 *p2*=0.5323	23.90±8.26 (n=4) *p1*=0.0209 *p2*=0.2195	52.25±15.31 (n=4) *p1*=0.0017 *p2*<0.0001
125	136.75±11.24 (n=4) *p1*<0.0001 *p2*=0.0043	49.00±15.25 (n=4) *p1*=0.0056 *p2*=0.2036	121.25±12.97 (n=4) *p1*<0.0001 *p2*=0.1172	19.80±7.30 (n=4) *p1*=0.0407 *p2*<0.0001	80.10±11.62 (n=4) *p1*=0.0001 *p2*=0.0008
150	138.75±11.44 (n=4) *p1*<0.0001 *p2*<0.0001	219.75±27.10 (n=4) *p1*<0.0001 *p2*=0.0720	116.25±15.73 (n=4) *p1*<0.0001 *p2*<0.0001	13.13±5.34 (n=4) *p1*=0.1457 *p2*<0.0001	177.75±22.32 (n=4) *p1*<0.0001 *p2*=0.0004
200	155.30±8.99 (n=4) *p1*<0.0001 *p2*<0.0001	170.75±24.06 (n=4) *p1*<0.0001 *p2*=0.0009	114.03±10.25 (n=4) *p1*<0.0001 *p2*<0.0001	20.13±7.62 (n=4) *p1*=0.0401 *p2*<0.0001	195.75±13.60 (n=4) *p1*<0.0001 *p2*<0.0001

Table IV. *Continued*

Table IV. *Continued*

Day	*Sp1*	*Ap1*	*Lysl Ox*	*IGFbp7*	*TLR4*
0	5.03±10.32 (n=4) p2=0.2002	–2.68±9.42 (n=4) p2=0.1105	3.00±19.11 (n=4) p2=0.4660	1.28±10.01 (n=4) p2=0.7981	2.55±9.04 (n=4) p2=0.1093
2	17.00±5.16 (n=4) p1=0.0832 p2=0.0001	22.48±6.19 (n=4) p1=0.0043 p2=0.0009	243.45±53.97 (n=4) p1=0.0002 p2=0.0024	–23.43±6.17 (n=4) p1=0.0057 p2=0.0001	–17.75±6.03 (n=4) p1=0.0097 p2=0.0012
14	104.25±19.62 (n=4) p1=0.0001 p2<0.0001	22.98±6.69 (n=4) p1=0.0044 p2=0.0667	197.00±13.52 (n=4) p1<0.0001 p2<0.0001	–12.30±6.23 (n=4) p1=0.0609 p2=0.0013	–16.10±4.75 (n=4) p1=0.0107 p2=0.0237
28	93.90±6.71 (n=4) p1<0.0001 p2<0.0001	–49.28±6.51 (n=4) p1=0.0002 p2=0.0588	164.50±9.88 (n=4) p1<0.0001 p2<0.0001	–16.18±6.11 (n=4) p1=0.0248 p2=0.0013	–16.33±6.20 (n=4) p1=0.0138 p2=0.0028
60	31.23±10.83 (n=4) p1=0.0128 p2<0.0001	–55.90±11.11 (n=4) p1=0.0003 p2=0.0093	124.23±13.38 (n=4) p1<0.0001 p2<0.0001	–15.50±6.65 (n=4) p1=0.0315 p2<0.0001	–26.75±9.00 (n=4) p1=0.0037 p2=0.0877
100	15.03±7.23 (n=4) p1=0.1635 p2=0.0001	–31.50±9.18 (n=4) p1=0.0047 p2<0.0001	126.00±14.94 (n=4) p1=0.0001 p2<0.0001	–7.98±13.97 (n=4) p1=0.3231 p2=0.0001	10.20±4.24 (n=4) p1=0.1764 p2=0.0038
125	68.03±7.55 (n=4) p1=0.0001 p2=0.0002	41.50±11.56 (n=4) p1=0.0010 p2=0.0003	107.75±24.74 (n=4) p1=0.0005 p2=0.0038	–9.00±10.42 (n=4) p1=0.2049 p2<0.0001	9.10±3.33 (n=4) p1=0.2229 p2=0.0001
150	219.50±50.35 (n=4) p1=0.0002 p2=0.0016	169.50±19.54 (n=4) p1<0.0001 p2=0.0001	139.53±11.81 (n=4) p1<0.0001 p2=0.0047	13.33±6.40 (n=4) p1=0.0888 p2=0.0001	9.65±14.45 (n=4) p1=0.4368 p2<0.0001
200	167.75±22.10 (n=4) p1<0.0001 p2=0.0027	145.25±11.03 (n=4) p1<0.0001 p2=0.0006	128.25±16.32 (n=4) p1=0.0001 p2=0.4167	9.73±2.58 (n=4) p1=0.1531 p2<0.0001	4.35±10.70 (n=4) p1=0.8058 p2<0.0001

Day	*TLR1*	*TLR2*	*TLR5*	*TLR6*	*TLR7*
0	5.67±8.62 (n=3) p2=0.5923	3.33±13.58 (n=3) p2=0.9499	6.20±4.53 (n=3) p2=0.8718	–1.13±16.56 (n=3) p2=0.5165	8.00±10.82 (n=3) p2=0.9663
2	299.67±30.11 (n=3) p1=0.0001 p2=0.0903	–17.67±7.02 (n=3) p1=0.0760 p2=0.5022	149.67±23.44 (n=3) p1=0.0005 p2=0.9622	357.67±19.01 (n=3) p1<0.0001 p2=0.0298	404.33±7.02 (n=3) p1<0.0001 p2=0.3076
14	68.03±10.87 (n=3) p1=0.0015 p2=0.1898	–50.00±17.52 (n=3) p1=0.0141 p2=0.7993	160.67±13.80 (n=3) p1=0.0001 p2=0.9321	504.33±8.50 (n=3) p1<0.0001 p2=0.3809	158.00±29.51 (n=3) p1=0.0012 p2=0.7595
28	116.67±26.35 (n=3) p1=0.0023 p2=0.8070	3.00±9.54 (n=3) p1=0.9739 p2=0.7163	122.00±18.68 (n=3) p1=0.0005 p2=0.9185	8.63±5.08 (n=3) p1=0.3841 p2=0.1873	116.33±11.02 (n=3) p1=0.0003 p2=0.5793
60	192.33±22.74 (n=3) p1=0.0002 p2=0.4617	–35.33±10.97 (n=3) p1=0.0185 p2=0.4008	80.67±7.02 (n=3) p1=0.0001 p2=0.4881	484.00±23.26 (n=3) p1<0.0001 p2=0.1460	9.33±17.79 (n=3) p1=0.9170 p2=0.6895
100	181.33±63.89 (n=3) p1=0.0092 p2=0.7475	–55.00±12.77 (n=3) p1=0.0056 p2=0.6364	26.33±8.33 (n=3) p1=0.0212 p2=0.4169	9.87±4.20 (n=3) p1=0.3273 p2=0.5263	191.67±7.64 (n=3) p1<0.0001 p2=0.1705
125	326.33±17.50 (n=3) p1<0.0001 p2=0.6255	227.00±20.95 (n=3) p1=0.0001 p2=0.8907	122.00±13.00 (n=3) p1=0.0001 p2=0.8985	16.00±8.54 (n=3) p1=0.1865 p2=0.3273	242.67±22.05 (n=3) p1=0.0001 p2=0.4178
150	140.33±36.35 (n=3) p1=0.0034 p2=0.7930	197.00±9.17 (n=3) p1<0.0001 p2=0.2039	285.33±17.16 (n=3) p1<0.0001 p2=0.3052	199.67±21.13 (n=3) p1=0.0002 p2=0.6455	902.00±23.30 (n=3) p1<0.0001 p2=0.2888
200	97.73±13.21 (n=3) p1=0.0005 p2=0.5166	216.33±8.08 (n=3) p1<0.0001 p2=0.8663	280.00±12.29 (n=3) p1<0.0001 p2=0.5722	220.00±21.63 (n=3) p1=0.0001 p2=0.7440	791.00±24.00 (n=3) p1<0.0001 p2=0.6121

Table IV. *Continued*

Table IV. *Continued*

Day	*Col1A*	*BRD1*	*BRD2*	*BRD3*	*BRD4*
0	6.50±8.81 (n=4)	1.50±12.71 (n=4)	0.48±13.10 (n=4)	0.73±16.21 (n=4)	1.50±10.14 (n=4)
	p2=1.0000	*p2*=0.2552	*p2*=0.3639	*p2*=0.4200	*p2*=0.2706
2	30.88±11.75 (n=4)	55.03±6.41 (n=4)	56.00±8.38 (n=4)	62.61±9.30 (n=4)	112.28±26.18 (n=4)
	p1=0.0160	*p1*=0.0003	*p1*=0.0004	*p1*=0.0006	*p1*=0.0002
	p2=0.0373	*p2*<0.0001	*p2*=0.0040	*p2*<0.0001	*p2*<0.0001
14	14.60±5.97 (n=4)	72.53±10.22 (n=4)	69.38±8.06 (n=4)	113.68±6.81 (n=4)	142.65±12.76 (n=4)
	p1=0.1789	*p1*=0.0001	*p1*=0.0001	*p1*<0.0001	*p1*<0.0001
	p2=.	*p2*<0.0001	*p2*=0.3589	*p2*<0.0001	*p2*<0.0001
28	14.03±7.09 (n=4)	64.25±5.84 (n=4)	50.63±7.62 (n=4)	56.98±7.20 (n=4)	121.55±12.14 (n=4)
	p1=0.2317	*p1*=0.0001	*p1*=0.0006	*p1*=0.0007	*p1*<0.0001
	p2=0.0048	*p2*<0.0001	*p2*=0.1059	*p2*<0.0001	*p2*<0.0001
60	16.63±6.20 (n=4)	60.23±11.46 (n=4)	63.13±10.22 (n=4)	61.93±10.80 (n=4)	111.43±10.64 (n=4)
	p1=0.1092	*p1*=0.0005	*p1*=0.0003	*p1*=0.0008	*p1*<0.0001
	p2=0.0027	*p2*=0.6721	*p2*=0.0001	*p2*=0.3621	*p2*<0.0001
100	12.53±1.76 (n=4)	62.80±15.01 (n=4)	80.75±10.47 (n=4)	89.75±16.60 (n=4)	120.25±8.77 (n=4)
	p1=0.2285	*p1*=0.0008	*p1*=0.0001	*p1*=0.0003	*p1*<0.0001
	p2=0.2482	*p2*<0.0001	*p2*=0.0463	*p2*=0.0038	*p2*=0.6064
125	15.53±3.35 (n=4)	87.25±15.06 (n=4)	61.05±7.76 (n=4)	97.23±12.03 (n=4)	130.75±21.23 (n=4)
	p1=0.1041	*p1*=0.0001	*p1*=0.0002	*p1*=0.0001	*p1*<0.0001
	p2=0.3618	*p2*=0.0823	*p2*=0.7967	*p2*<0.0001	*p2*<0.0001
150	11.43±6.01 (n=4)	72.18±9.19 (n=4)	31.50±11.10 (n=4)	52.50±16.01 (n=4)	155.00±15.41 (n=4)
	p1=0.3915	*p1*=0.0001	*p1*=0.0112	*p1*=0.0039	*p1*<0.0001
	p2=0.2250	*p2*<0.0001	*p2*=0.0002	*p2*<0.0001	*p2*<0.0001
200	5.05±15.35 (n=4)	81.25±11.03 (n=4)	70.25±20.42 (n=4)	90.53±8.77 (n=4)	143.50±15.80 (n=4)
	p1=0.8753	*p1*=0.0001	*p1*=0.0012	*p1*=0.0001	*p1*<0.0001
	p2<0.0001	*p2*<0.0001	*p2*=0.0013	*p2*<0.0001	*p2*<0.0001

Data summary using mean±SD and group comparisons, where *p1* is the *p*-value for the comparison of gene expression in lungs of C3H/HeNHsd mice between each day and day 0 for the corresponding gene, *p2* is the *p*-value for the comparison between C57BL/6NHsd mice and C3H/HeNHsd mice at the corresponding day for the corresponding gene. All these *p*-values were calculated with the two-sided two-sample *t*-test.

Table V. *Analysis of western blot data from C57BL/6NHsd and C3H/HeNHsd mouse lung.*

Mouse type	Day	MnSOD	NFKB	Collagen-1a	BRD4
C57BL/6NHsd	0	1±0 (n=4)	1±0 (n=4)	1±0 (n=3)	1±0 (n=2)
	2	2.18±1.43 (n=4)	0.89±0.30 (n=4)	0.73±0.60 (n=3)	0.84±0.51 (n=2)
		p1=0.1977	*p1*=0.5331	*p1*=0.5157	*p1*=0.7305
	75	2.20±0.92 (n=4)	1.19±0.80 (n=4)	1.60±1.31 (n=3)	0.31±0.22 (n=2)
		p1=0.0814	*p1*=0.6639	*p1*=0.5076	*p1*=0.1400
	150	2.64±2.07 (n=4)	2.20±1.15 (n=4)	4.32±1.98 (n=3)	0.69±0.16 (n=2)
		p1=0.2126	*p1*=0.1271	*p1*=0.1011	*p1*=0.2206
C3H/HeNHsd	0	1±0 (n=4)	1±0 (n=4)	1±0 (n=3)	1±0 (n=2)
	2	0.94±0.34 (n=4)	0.63±0.25 (n=4) 1	0.77±0.61 (n=3)	2.00±0.71 (n=2)
		p1=0.7366 *p2*=0.1804	*p1*=0.0611 *p2*=0.228	*p1*=0.5865 *p2*=0.9342	*p1*=0.2952 *p2*=0.2005
	60	1.15±0.39 (n=4)	1.02±0.12 (n=4)	0.64±0.74 (n=3)	7.00±4.24 (n=2)
		p1=0.5022 *p2*=0.0820	*p1*=0.7486 *p2*=0.7006	*p1*=0.4850 *p2*=0.3273	*p1*=0.2952 *p2*=0.1559
	150	1.27±0.54 (n=4)	0.70±0.21 (n=4)	0.62±0.55 (n=3)	5.50±1.56 (n=2)
		p1=0.3907 *p2*=0.2494	*p1*=0.0638 *p2*=0.0767	*p1*=0.3599 *p2*=0.0358	*p1*=0.1526 *p2*=0.0489

Data are summarized with mean±SD. P1 is the *p*-value for the comparison between each day and day 0 for each gene and each mouse type, using the two-sided one-sample *t*-test. *P2* is the *p*-value for the comparison between the two mouse strains for each gene at each day, using the two-sided two-sample *t*-test.

Table VI. *Percentage of DNA promoter methylation for 6 representative genes in the lungs of 20-Gy thoracic irradiated C57BL/6NHsd mice.*

Day	*TGFb*	*SOD2*	*FGF1*	*VEGFa*	*CTGF*	*IGFbp7*
0	96.25±0.90 (n=4)	92.65±1.18 (n=4)	96.71±0.64 (n=4)	95.10±0.77 (n=4)	93.93±0.87 (n=4)	95.23±0.73 (n=4)
2	98.88±0.40 (n=4) *p*=0.0018	98.35±0.54 (n=4) *p*=0.0001	98.81±0.36 (n=4) *p*=0.0013	98.50±0.84 (n=4) *p*=0.0010	99.40±0.29 (n=4) *p*<0.0001	81.84±1.68 (n=4) *p*<0.0001
14	88.28±2.39 (n=4) *p*=0.0008	89.53±4.07 (n=4) *p*=0.1908	92.50±2.38 (n=4) *p*=0.0143	98.78±0.30 (n=4) *p*=0.0001	97.80±0.55 (n=4) *p*=0.0003	81.75±1.50 (n=4) *p*<0.0001
28	84.45±3.39 (n=4) *p*=0.0005	90.00±2.16 (n=4) *p*=0.0749	91.40±2.33 (n=4) *p*=0.0046	98.70±0.55 (n=4) *p*=0.0003	97.53±0.49 (n=4) *p*=0.0004	82.50±2.38 (n=4) *p*=0.0001
75	75.08±3.15 (n=4) *p*<0.0001	80.75±3.30 (n=4) *p*=0.0005	86.63±0.97 (n=4) *p*<0.0001	99.00±0.26 (n=4) *p*=0.0001	97.00±0.92 (n=4) *p*=0.0028	83.96±1.89 (n=4) *p*<0.0001
100	76.45±1.63 (n=4) *p*<0.0001	86.00±1.88 (n=4) *p*=0.0010	88.08±2.26 (n=4) *p*=0.0003	98.30±0.48 (n=4) *p*=0.0004	98.00±0.64 (n=4) *p*=0.0003	90.85±1.74 (n=4) *p*=0.0035
150	96.83±0.64 (n=4) *p*=0.3378	97.40±0.72 (n=4) *p*=0.0005	95.88±1.17 (n=4) *p*=0.2582	98.98±0.51 (n=4) *p*=0.0002	99.43±0.43 (n=4) *p*<0.0001	97.78±1.34 (n=4) *p*=0.0156
200	98.20±0.55 (n=4) *p*=0.0101	98.23±0.53 (n=4) *p*=0.0001	96.38±0.87 (n=4) *p*=0.5603	98.43±0.46 (n=4) *p*=0.0003	99.08±0.33 (n=4) *p*<0.0001	98.30±0.39 (n=4) *p*=0.0003

Data summary using mean±SD and group comparisons for methylation data, where *p* is the *p*-value for the comparison of DNA promoter methylation percentage for the corresponding gene in lungs of C57BL/6NHsd mice between each day and day 0, using the two-sided two-sample *t*-test.

Table VII. *Percentage of DNA promoter methylation for 6 representative genes in the lungs of 20-Gy thoracic irradiated C3H/HeNHsd mice.*

Day	*TGFb*	*SOD2*	*FGF1*	*VEGFa*	*CTGF*	*IGFbp7*
0	92.45±1.97 (n=4) *p2*=0.0127	93.45±1.05 (n=4) *p2*=0.3512	95.43±1.51 (n=4) *p2*=0.1685	89.88±0.97 (n=4) *p2*=0.0002	94.93±0.79 (n=4) *p2*=0.1401	95.60±0.56 (n=4) *p2*=0.4542
2	90.78±1.93 (n=4) *p1*=0.2695 *p2*=0.0027	91.28±0.75 (n=4) *p1*=0.0153 *p2*<0.0001	94.45±0.44 (n=4) *p1*=0.2606 *p2*<0.0001	95.25±0.37 (n=4) *p1*<0.0001 *p2*=0.0004	96.75±0.24 (n=4) *p1*=0.0045 *p2*<0.0001	94.50±0.42 (n=4) *p1*=0.0197 *p2*=0.0004
14	95.23±0.86 (n=4) *p1*=0.0415 *p2*=0.0015	91.55±0.60 (n=4) *p1*=0.0201 *p2*=0.3948	94.40±0.61 (n=4) *p1*=0.2536 *p2*=0.2093	95.95±0.26 (n=4) *p1*<0.0001 *p2*<0.0001	97.45±0.37 (n=4) *p1*=0.0012 *p2*=0.3302	94.00±0.62 (n=4) *p1*=0.0085 *p2*<0.0001
28	91.35±0.54 (n=4) *p1*=0.3229 *p2*=0.0251	95.45±0.54 (n=4) *p1*=0.0150 *p2*=0.0123	92.85±0.31 (n=4) *p1*=0.0391 *p2*=0.3016	96.35±0.44 (n=4) *p1*<0.0001 *p2*=0.0006	97.85±0.34 (n=4) *p1*=0.0005 *p2*=0.3156	94.93±0.43 (n=4) *p1*=0.1037 *p2*=0.0015
75	91.05±0.83 (n=4) *p1*=0.2383 *p2*=0.0001	96.43±0.42 (n=4) *p1*=0.0019 *p2*=0.0022	94.40±0.43 (n=4) *p1*=0.2387 *p2*<0.0001	96.28±0.44 (n=4) *p1*<0.0001 *p2*<0.0001	97.63±0.53 (n=4) *p1*=0.0013 *p2*=0.2840	94.88±0.33 (n=4) *p1*=0.0672 *p2*=0.0011
100	87.50±3.11 (n=4) *p1*=0.0360 *p2*=0.0007	95.43±0.46 (n=4) *p1*=0.0138 *p2*=0.0014	94.20±0.77 (n=4) *p1*=0.1982 *p2*=0.0021	96.68±1.00 (n=4) *p1*=0.0001 *p2*=0.0268	96.88±0.93 (n=4) *p1*=0.0188 *p2*=0.0928	93.35±0.54 (n=4) *p1*=0.0012 *p2*=0.0336
150	91.10±2.11 (n=4) *p1*=0.3853 *p2*=0.0020	97.83±0.91 (n=4) *p1*=0.0008 *p2*=0.4908	94.98±1.01 (n=4) *p1*=0.6372 *p2*=0.2874	97.20±0.70 (n=4) *p1*<0.0001 *p2*=0.0063	96.28±0.81 (n=4) *p1*=0.0551 *p2*=0.0005	92.60±0.95 (n=4) *p1*=0.0016 *p2*=0.0007
200	90.60±1.27 (n=4) *p1*=0.1656 *p2*<0.0001	98.33±0.51 (n=4) *p1*=0.0002 *p2*=0.7955	94.10±0.65 (n=4) *p1*=0.1572 *p2*=0.0056	97.50±0.63 (n=4) *p1*<0.0001 *p2*=0.0545	97.33±0.36 (n=4) *p1*=0.0015 *p2*=0.0004	91.28±0.53 (n=4) *p1*<0.0001 *p2*<0.0001

Data summary using mean±SD and group comparisons for percent methylation, where p1 is the p-value for the comparison of DNA promoter methylation percentage for the corresponding gene in the lungs of C3H/HeNHsd mice between each day and day 0, p2 is the *p*-value for the comparison of DNA promoter methylation percentage between C57BL/6NHsd mice and C3H/HeNHsd mice at the corresponding day for the corresponding gene. All *p*-values were calculated with the two-sided two sample *t*-test.

Changes in levels of CpG methylation in the gene promoter(s) for TGFβ, MnSOD (SOD2), FGF1, and, IGFbp7 correlate with levels of gene transcripts in irradiated mouse lungs. We next determined if increases in specific gene transcript levels correlated with de-methylation of the promoters for those genes. In lung tissue from C57BL/6NHsd mice irradiated to 20 Gy, inflammation-associated genes (*Tgfb* and *Sod2*) showed significant promoter de-methylation (<3% methylation) during both the acute and late stages, and increased methylation (25.67% and 20.67%, respectively) during the latent period (Figure 7). De-methylation of the *Tgfb* promoter in C57BL/6NHsd mouse lung was consistent with elevated levels of gene transcripts for *Tgfb*. In contrast, in lung tissue from C3H/HeNHsd mice, the promoter for the *Tgfb* gene showed significantly greater methylation during the late phase (days 150 and 200), concordant with lower levels of *Tgfb* transcript and absence of histopathological evidence of pulmonary fibrosis (Figure 7) (Table VI).

The *MnSOD* CpG gene promoter methylation levels were similar in the lung tissues of both C57BL/6NHsd and C3H/HeNHsd mice irradiated to 20 Gy, concordant with the observed similar levels of MnSOD transcripts (Figure 7B).

Levels of de-methylation of the CPG promoters for *Fgf-1* (Figure 7C) and *Igfbp7* (Figure 7D) were also concordant with the relative levels of transcripts. In C57BL/6NHsd mouse lung, the CpG promoter for the *Igfbp7* gene showed stable methylation during the acute and latent period (19% and 17%, respectively), followed by significant de-methylation (<2% methylation) (Figure 7D) during the late fibrosis stage consistent with increased transcript levels (Figure 7C) (Table VI).

In C57BL/6NHsd mice, CpG promoters for the *Vegf* and *Ctgf* gene showed significant de-methylaton (<4% methylation) at day 150 following irradiation, consistent with levels of transcripts (Table VI). In contrast, lung tissue of C3H/HeNHsd mice irradiated to 20 Gy showed *VEGF* and *CTGF* gene promoters had lower levels of de-methylation consistent with the low levels of transcripts in these lung tissues. Therefore, levels of de-methylation of specific gene promoters in lung tissue correlated with increased gene transcript levels for those same genes over 200 days after 20 Gy irradiation in both pulmonary fibrosis-prone C57BL/6NHsd and fibrosis-resistant C3H/HeNHsd mice.

Discussion

In the present study, we measured levels of RNA transcripts for 25 genes in the lungs of irradiated C3H/HeNHsd mice compared to C57BL/6NHsd mice. C57BL/6NHsd mice showed bi-phasic early and late increase in expression of *NFkβ, Nrf2, Sod2, Tgfb, Fgf-1, Sp-1* and *Ap-1* separated by a time period when levels were reduced. While C3H/HeNHsd mice also demonstrated irradiation-induced elevation of *NFkβ, Sp1*, and *Ap1*, levels of MnSOD, *Tgfb*, and *Fgf-1* were lower. Prior studies showed that relative levels of irradiated whole-lung RNA transcripts correlated with levels in separated endothelial and epithelial cells (25); therefore, we did not separate these cell populations for the comparison of irradiation-induced lung transcripts between these two mouse strains. Twenty percent of C3H/HeNHsd mice irradiated to 20 Gy to the thoracic cavity died rapidly, suggesting esophagitis or liver damage; however, no histopathological evidence of injury to these organs was detected. Since gene transcript elevations in lower-irradiation dose groups of C3H/HeNHsd mice were similar to the 20-Gy irradiation group, we compared the 80% lung irradiation survivors after 20 Gy in an attempt to detect differences in the response of the lung in this strain, which did not lead to the pulmonary fibrosis observed in 20 Gy irradiated C57BL/6NHsd mice.

There was prominent late elevation of RNA transcripts for *Tlr4* and *Igfbp7* in the lungs from irradiated C57BL/6NHsd mice compared to low levels at the same late time points in C3H/HeNHsd mice. Macrophage TLR4 elevation occurs during lung inflammation (36-42), and promotes hepatic (43), and renal fibrosis (37). The low level of *TLR4* expression in irradiated C3H/HeNHsd mouse lung is consistent with prior data showing that low *TLR4* levels ameliorate pulmonary (41) and renal fibrosis (37, 44). However, other data report different patterns of TLR4 expression. One report showed that both TLR4 and TLR2 were required to induce pulmonary fibrosis (38). Another report showed that TLR4 elevation prevented bleomycin fibrosis (41). A mutation on exon 3 of the *TLR4* gene in C3H/HeNHsd mice was associated with infection and aberrant graft *versus* host disease responses, but these mice were still fibrosis-resistant (42). Since fibrosis resistance in C3H/HeNHsd mice appears to be independent of levels of TLR4, it is unlikely that TLR4 is the single critical regulator of irradiation pulmonary fibrosis.

Igfbp7 transcript levels were increased in the irradiation-induced fibrotic lungs of C57BL/6NHsd mice. This cell adhesion molecule promotes inflammation (45, 46), is elevated in human sclerodermatous lungs and in lungs of patients with lung transplant rejection (28), and in idiopathic pulmonary fibrosis (47), and abnormal wound repair. IGFbp7 down-modulates insulin-like growth factor 1 receptor, and inhibits cell growth and angiogenesis (8). IGFbp7 levels have been shown to correlate with slowed tumor progression suggesting that proliferating myofibroblasts in tumors and in fibrotic lungs of C57BL/6NHsd mice may also be examples of tissue responses in that strain (45-48).

A major observed difference between mouse strains was in the pulmonary levels of transcripts for bromodomain epigenetic reader proteins Brd1-4. Bromodomain epigenetic reader proteins bind to the acetylated lysine group of histone 4 (49) and modulate expression of genes including NFkb (33, 50-56). These gene products can induce fibrosis (33) and alter cell-cycle progression (57). Elevation of *Brd1-4* transcripts in the lungs of C57BL/6NHsd mice during the period between the acute and fibrosis phases correlated with the time of decreased *Tgfb, Tnfa, Nfkb,* and *Nrf2*. Decrease in bromodomain gene transcripts in C57BL/6NHsd mice at days 150-200 correlated with elevated levels of collagen 1a, *Tgfb*, and *Tlr4*, and in other studies (24) coincided with the time of both histopathological lung fibrosis and bone marrow stromal cell homing to lungs. In contrast, stably-elevated levels of *Brd1-4* over 200 days post-irradiation in C3H/HeNHsd mice correlated with decreased levels of transcripts for *Vwf* and *Vegf*.

BET bromodomain proteins, Brd2-4, are known to be associated with histones through mitotic divisions (32, 57). Our observation of low levels of *Brd1-4* during fibrosis is inconsistent with prior publications showing that elevation of Brd1-4 causes fibrosis (32-33). Our data are also inconsistent with those showing that low levels of Brd1-4 down-regulate *TLR4* (50-52, 58), which was elevated in irradiated C57BL/6NHsd mouse lungs at 150 days. Brd4 binds to and up-regulates the promoter for the gene for the fibrogenic cytokine Il6 (52, 55), and activates *NFkb*, which is also up-regulated during radiation fibrosis. Our data are consistent with a publication showing that Brd4 elevation inhibits bleomycin lung fibrosis in C57BL/6NHsd mice (33). This data is also consistent with our demonstration that Brd1-4 levels are elevated in irradiated fibrosis-resistant C3H/HeNHsd mice. Studies with a small-molecule inhibitor of BRD proteins, should allow for testing of the hypothesis that irradiation-induced lung fibrosis can be initiated in C3H/HeNHsd mice by reducing Brd1-4 levels (59).

Irradiation pulmonary fibrosis has been linked to elevated levels of TGFβ1 (7, 60-61), IL6 (9, 10) increased binding of NFϰB and AP1 to the chemokine ligand 2 promoter (16), IGFBP-3 (13), and to the induction of extracellular matrix protein Tenascin (14, 16). Irradiated C57BL/6NHsd mice are known to display increased lung levels of TGFβ (17, 24), but also showed greater levels of irradiation-induced apoptosis in thymocytes and intestinal crypts (62). C57BL/6NHsd mice are prone to bleomycin-induced (18, 20, 22, 63), as well as irradiation-induced, lung (31) and intestinal (62) fibrosis. In contrast, C3H/HeNHsd mice are known to resist not only irradiation-induced pulmonary fibrosis (31), but also fibrosis caused by bleomycin (38), silica (64), ozone (65-66), and hyperoxia (67). Mouse strain-specific propensity for radiation fibrosis was not correlated with *in vitro* fibroblast radiosensitivity, suggesting that a paracrine or indirect mechanism of cell signaling is involved *in vivo* (31). We did not detect differences in the histopathology of cardiac tissues between irradiated mouse strains, and injected luc+ stromal cell progenitors of fibrosis-associated areas of the lung did not home to the heart (25); however, differences in physiological cardiac response to thoracic irradiation may be involved in the etiology of both rapid death of C3H/HeNHsd mice and fibrosis in lungs of C57BL/6NHsd mice.

While some molecular biological pathways are common to multiple etiologies of pulmonary fibrosis (38, 52, 57), the present data revealed unique signatures associated with the onset of radiation pulmonary fibrosis in C57BL/6NHsd mice: prominently elevated *Tlr4* and a drop in transcripts and protein for the *Brd4* epigenetic reader protein. Further studies are required to elucidate the potential interactive role of these elevated or decreased gene transcripts in the mechanism of irradiation pulmonary fibrosis.

Acknowledgements

This study was supported by NIH grants CA-R01-CA119927 and NIAID U19-A1068021. This project used the UPCI animal facility that is supported in part by award P30CA047904.

References

1 Kim TH, Cho KH, Pyo HR, Lee JS, Zo JI, Lee DH, Lee JM, Kim HY, Hwangbo B, Park SY, Kim JY, Shin KH and Kim DY: Dose-volumetric parameters for predicting severe radiation pneumonitis after three-dimensional conformal radiation therapy for lung cancer. Radiology *234*: 208-215, 2005.

2 Dang J, Li G, MaL, Diao R, Zang S, Han C, Zhang S and Yao L: Predictors of grade >2 and grade >3 radiation pneumonitis in patients with locally advanced non-small cell lung cancer treated with three-dimensional conformal radiotherapy. Acta Oncol *52(6)*: 1175-1180, 2013.

3 Parashar B, Edwards A, Mehta R, Pasmantier M, Wernicke AG, Sabbas A, Kerestez RS, Nori D and Chao KS: Chemotherapy significantly increases the risk of radiation pneumonitis in radiation therapy of advanced lung cancer. Am J Clin Oncol *34*: 160-164, 2011.

4 Ruben P and Casarett GW: Clinical Radiation Pathology. Philadelphia, Saunders, 1968.

5 Williams JP, Johnston CJ and Finkelstein JN: Treatment for radiation-induced pulmonary late effects: Spoiled for choice or looking in the wrong direction? Curr Drug Targets *11*: 1386-1394, 2010.

6 Movsas B, Raffin TA, Epstein AH and Link CJ Jr.: Pulmonary radiation injury. Chest *111*: 1061-1076, 1997.

7 Anscher MS: Targeting the TGF-β1 pathway to prevent normal tissue injury after cancer therapy. Oncologist *15(4)*: 350-359, 2010.

8 Chen D, Yoo BK, Santhekadur PK, Gredler R, Bhutia SK, Das SK, Fuller C, Su ZZ, Fisher PB and Sarkar D: Insulin-like growth factor-binding protein-7 functions as a potential tumor suppressor in hepatocellular carcinoma. Clin Cancer Res *17(21)*: 6693-6701, 2011.

9 Chen Y, Rubin P, Williams J, Hernady E, Smudzin T and Okunieff P: Circulating IL-6 as a predictor of radiation pneumonitis. Int J Radiat Oncol Biol Phys *49(3)*: 641-648, 2001.

10 Arpin D, Perol D, Blay JY, Falchero L, Claude L, Vuillermoz-Blas S, Martel-Lafay I, Ginestet C, Alberti L, Nosov D, Etienne-Mastroianni B, Cottin V, Perol M, Guerin JC, Cordier JF and Carrie C: Early variations of circulating interleukin-6 and interleukin-10 levels during thoracic radiotherapy are predictive for radiation pneumonitis. J Clin Onc *23(34)*: 8748-8756, 2005.

11 Mazeron R, Etienne-Mastroianni B, Perol D, Arpin D, Vincent M, Falchero L, Martel-Lafay I, Carrie C and Claude L: Predictive factors of late radiation fibrosis: A prospective study in non-small cell lung cancer. Int J Radiat Oncol Biol Phys *77(1)*: 38-43, 2007.

12 Moeller A, Rodriguez-Lecompte JC, Wang L, Gauldie J and Kolb M: Models of pulmonary fibrosis. Drug Discov Today: Disease Models *3*: 243-249, 2006.

13 Brissett M, Veraldi KL, Pilewski JM, Medsger TA Jr. and Feghali-Bostwick CA: Localized expression of tenascin in systemic sclerosis-associated pulmonary fibrosis and its regulation by insulin-like growth factor-binding protein 3. Arthritis Rheum *64(1)*: 272-280, 2012.

14 Wehrhan F, Rodel F, Grabenbauer GG, Amann K, Bruckl W, Schultze-Mosgau S: Transforming growth factor beta 1-dependent regulation of tenascin-C in radiation-impaired wound healing. Radiother Oncol *72*: 297-303, 2004.

15 Rosiello RA and Merrill WW: Radiation-induced lung injury. Clin Chest Med *11(1)*: 65-71, 1990.

16 Deng X, Xu M, Yuan C, Yin L, Chen X, Zhou X, Li G, Fu Y, Feghali-Bostwick CA, Pang L: Transcriptional regulation of increased CCL2 expression in pulmonary fibrosis involves nuclear factor-KB and activator protein-1. Int J Biochem Cell Biol *45(7)*: 1366-1376, 2013.

17 Johnston CJ, Piedboeuf B, Baggs R, Rubin P, Finkelstein JN: Differences in correlation of mRNA gene expression in mice sensitive and resistant to radiation-induced pulmonary fibrosis. Radiat Res *142(2)*: 197-203, 1995.

18 Haston C and Travis E: Murine susceptibility to radiation-induced pulmonary fibrosis is influenced by a genetic factor implicated in susceptibility to bleomycin-induced pulmonary fibrosis. Cancer Res *57*: 5286-5291, 1997.

19 Franko AJ, Sharplin J, Ward WF and Taylor JM: Evidence for two patterns of inheritance of sensitivity to induction of lung fibrosis in mice by radiation, one of which involves two genes. Radiat Res *146*: 68-74, 1996.

20 Haston CK, Zhou X, Gumbiner-Russo L, Irani R, Dejournett R, Gu X, Weil M, Amos CI and Travis EL: Universal and radiation-specific loci influence murine susceptibility to radiation-induced pulmonary fibrosis. Cancer Res *62(13)*: 3782-3788, 2002.

21 Jackson IL, Xu P, Hadley C, Katz BP, McGurk R, Down JD and Vujaskovic Z: A preclinical rodent model of radiation-induced lung injury for medical countermeasure screening in accordance with the FDA animal rule. Health Phys *103(4)*: 463-473, 2012.

22 Haston CK, Wang M, Dejournett RE, Zhou X, Ni D, Gu X, King TM, Weil MM, Newman RA, Amos CI, Travis EL: Bleomycin hydrolase and a genetic locus within the MHC affect risk for pulmonary fibrosis in mice. Hum Mol Genet *11(16)*: 1855-1863, 2002.

23 Epperly M, Guo H, Gretton JE and Greenberger JS: Bone marrow origin of myofibroblasts in irradiation pulmonary fibrosis. Am J Respir Cell Mol Biol *29*: 213-224, 2003.

24 Kalash R, Epperly MW, Goff J, Dixon T, Sprachman MM, Zhang X, Shields D, Cao S, Franicola D, Wipf P, Berhane H, Wang H, Au J and Greenberger JS: Amelioration of irradiation pulmonary fibrosis by a water-soluble bi-functional Sulfoxide radiation mitigator (MMS350). Radiat Res *180(5)*: 474-490, 2013.

25 Kalash R, Berhane H, Goff J, Houghton F, Epperly MW, Dixon T, Zhang X, Sprachman MM, Wipf P, Franicola D, Wang H and Greenberger JS: Thoracic irradiation effects on pulmonary endothelial compared to alveolar type II cells in fibrosis prone C57BL/6NTac mice. In Vivo *27*: 291-298, 2013.

26 Paris F, Fuks Z, Kang A, Capodieci P, Juan G, Ehleiter D, Haimovitz-Freidman A, Cordon-Cardo C and Kolesnick R: Endothelial apoptosis as the primary lesion initiating intestinal radiation damage in mice. Science *293*: 293-297, 2001.

27 Epperly MW, Travis EL, Sikora C and Greenberger JS: Magnesium superoxide dismutase (MnSOD) plasmid/liposome pulmonary radioprotective gene therapy: Modulation of irradiation-induced mRNA for IL-1, TNF-α, and TGF-β correlates with delay of organizing alveolitis/fibrosis. Biology of Blood and marrow Transplantation *5*: 204-214, 1999.

28 Hsu E, Shi H, Jordan RM, Lyons-Weiler J, Pilewski JM and Feghali-Bostwick CA: Lung tissues in patients with systemic sclerosis have gene expression patterns unique to pulmonary fibrosis and pulmonary hypertension. Arthritis Rheum *63(3)*: 783-794, 2011.

29 Paun A, Fox J, Balloy V, Chignard M, Qureshi ST and Haston CK: Combined Tlr2 and Tlr4 deficiency increases radiation-induced pulmonary fibrosis in mice. Int J Radiat Oncol Biol Phys *77(4)*: 1198-1205, 2010.

30 Pulskens W, Rampanelli E, Teske GJ, Butter LM, Claessen N, Luirink IK, van der Poll T, Florquin S and Leemans JC: TLR4 promotes fibrosis but attenuates tubular damage in progressive renal injury. J Am Soc Nephrol *21(8)*: 1299-1308, 2010.

31 Dileto CL and Travis EL: Fibroblast radiosensitivity *in vitro* and lung fibrosis *in vivo*: comparison between a fibrosis-prone and fibrosis-resistant mouse strain. Radiat Res *146(1)*: 61-67, 1996.

32 Tang X, Peng R, Phillips JE, Deguzman J, Ren Y, Apparsundaram S, Luo Q, Bauer CM, Fuentes ME, DeMartino JA, Tyagi G, Garrido R, Hogaboam CM, Denton CP, Holmes AM, Kitson C, Stevenson CS and Bud DC: Assessment of Brd4 inhibition in idiopathic pulmonary fibrosis lung fibroblasts and *in vivo* models of lung fibrosis. Am J Pathol *183(2)*: 470-479, 2013.

33 Tang X, Peng R, Ren Y, Apparsundaram S, Deguzman J, Bauer CM, Hoffman AF, Hamilton S, Liang Z, Zeng H, Fuentes ME, Demartino JA, Kitson C, Stevenson CS and Budd DC: BET bromodomain proteins mediate downstream signaling events following growth factor stimulation in human lung fibroblasts and are involved in bleomycin-induced pulmonary fibrosis. Mol Pharmacol *83*: 283-293, 2013.

34 Rajagopalan MS, Stone B, Rwigema JC, Salimi U, Epperly MW, Goff J, Franicola D, Dixon T, Cao S, Zhang X, Buchholz BM, Bauer AJ, Choi S, Bakkenist C, Wang H and Greenberger JS: Intraesophageal manganese superoxide dismutase-plasmid liposomes ameliorates novel total body and thoracic irradiation sensitivity of homologous deletion recombinant negative nitric oxide synthase-1 (NOS–/–) mice. Radiat Res *174*: 297-312, 2010.

35 He Z, Zhu Y and Jiang H: Inhibiting toll-like receptor 4 signaling ameliorates pulmonary fibrosis during acute lung injury induced by lipopolysaccharide: An experimental study. Respir Res *10*: 126, 2009.

36 Stramer BM, Mori R and Martin P: The inflammation-fibrosis link? A Jekyll and Hyde role for blood cells during wound repair. J Invest Dermatol *127*: 1009-1017, 2007.

37 Wynn TA: Cellular and molecular mechanisms of fibrosis. J Pathol *214*: 199-210, 2008.

38 Paun A, Lemay AM and Haston CK: Gene expression profiling distinguishes radiation-induced fibrosing alevolitis from alveolitis in mice. Radiat Res *173(4)*: 512-521, 2010.

39 Imado T, Iwasaki T, Kitano S, Santake A, Kuroiwa T, Tsunemi S and Sano H: The protective role of host Toll-like receptor-4 in acute graft-versus-host disease. Transplantation *90(10)*: 1063-1070, 2010.

40 Margaritopoulos GA, Antoniou KM, Karagiannis K, Samara KD, Lasithiotaki I, Vassalou E, Lymbouridou R, Koutala H and Siafakas NM: Investigation of Toll-like receptors in the pathogenesis of fibrotic and granulomatous disorders: A bronchoalveolar lavage study. Fibrogenesis Tissue Repair *3*: 20, 2010.

41 Yang H-Z, Wang JP, Mi S, Liu HZ, Cui B, Yan HM, Yan J, Li Z, Liu H, Hua F, Lu W and Hu ZW: TLR4 activity is required in the resolution of pulmonary inflammation and fibrosis after acute and chronic lung injury. Am J Pathol *180(1)*: 274-292, 2012.

42 Poltorak A, He X, Smirnova I, Liu MY, Van Huffel C, Du X, Birdwell D, Alejos E, Silva M, Galanos C, Freudenberg M, Ricciardi-Castagnoli P, Layton B and Beutler B: Defective LPS signaling in C3H/HeJ and C57BL/10ScCr mice: Mutations in *Tlr4* gene. Science *282(5396)*: 2085-2088, 1998.
43 Seki E, De Minicis S, Osterreicher CH, Kluwe J, Osawa Y, Brenner DA and Schwabe RF: TLR4 enhances TGF-beta signaling and hepatic fibrosis. Nat Med *13(11)*: 1324-1332, 2007.
44 LeBleu VS, Taduri G, O'Connell J, Teng Y, Cooke VG, Woda C, Sugimoto H and Kalluri R: Origin and function of myofibroblasts in kidney fibrosis. Nat Med *19(8)*: 1047-1052, 2013.
45 Herman JG and Baylin SB: Gene silencing in cancer in association with promoter hypermethylation. N Engl J Med *349*: 2042-2054, 2003.
46 Darr J, Klochendler A, Isaac S, Eden A: Loss of IGFBP7 expression and persistent AKT activation contribute to SMARCB1/Snf5-mediated tumorigenesis. Oncogene doi: 10.1038/onc.2013.261, 2013.
47 Allen JT, Knight RA, Bloor CA, Spiteri MA: Enhanced insulin-like growth factor binding protein-related protein 2 (connective tissue growth factor) expression in patients with idiopathic pulmonary fibrosis and pulmonary sarcoidosis. Am J Resp Cell Mol Biol *21(6)*: 693-700, 1999.
48 Chen Z, Lu F, Fang H and Huang H: Effect of mesenchymal stem cells on renal injury in rats with severe acute pancreatitis. Exp Biol Med *238*: 687-695, 2013.
49 Zeng L and Ming-Ming Z: Bromodomain: An acetyl-lysine binding domain. FEBS Lett *513*: 124-128, 2002.
50 Zhang G, Liu R, Zhong Y, Plotnikov AN, Zhang W, Zeng L, Rusinova E, Gerona-Nevarro G, Moshkina N, Joshua J, Chuang PY, Ohlmeyer M, He JC and Zhou MM: Down-regulation of NF-kb transcriptional activity in HIV activity in HIV-associated kidney disease by BRD4 inhibition. J Biol Chem *287*: 28840-28851, 2012.
51 Zhang W, Prakash C, Sum C, Gong Y, Li Y, Kwok JJ, Thiessen N, Pettersson S, Jones SJ, Knapp S, Yang H and Chin KC: Bromodomain-containing protein 4 (BRD4) regulates RNA polymerase II serine 2 phosphorylation in human $CD4^+$ T-cells. J Biol Chem *287(51)*: 43137-43155, 2012.
52 Belkina AC, Nikolajczyk BS and Denis GV: BET protein function is required for inflammation: Brd2 genetic disruption and BET inhibitor JQ1 impair mouse macrophage inflammatory responses. J Immunol *190(7)*: 3670-3678, 2013.
53 Belkina AC and Denis GV: BET domain co-regulators in obesity, inflammation, and cancer. Nat Rev Cancer *12(7)*: 465-477, 2012.
54 Nicodeme E, Jeffrey KL, Schaefer U, Beinke S, Dewell S, Chung CW, Chandwani R, Marazzi I, Wilson P, Coste H, White J, Kirilovsky J, Rice CM, Lora JM, Prinjha RK, Lee K and Tarakhovsky A: Suppression of inflammation by a synthetic histone mimic. Nature *468*: 1119-1123, 2010.
55 Muller S, Filippakopoulos P and Knapp S: Bromodomains as therapeutic targets. Expert Rev Mol Med *13*: e29, 2011.
56 Huang B, Yang XD, Zhou MM, Ozato K and Chen LF: Brd4 coactivates transcriptional activation of NF-kappaB via specific binding to acetylated RE1A. Mol Cell Biol *29(5)*: 1375-1387, 2009.
57 Tsukui T, Ueha S, Abe J, Hashimoto S, Shichino S, Shimaoka T, Shand FH, Arakawa Y, Oshima K, Hattori M, Inagaki Y, Tomura M and Matsushima K: Qualitative rather than quantitative changes are hallmarks of fibroblasts in bleomycin-induced pulmonary fibrosis. Am J Pathol *183(3)*: 758-773, 2013.
58 Lockwood WW, Zejnullahu K, Bradner JE and Varmus H: Sensitivity of human lung adenocarcinoma cell lines to targeted inhibition of BET epigenetic signaling proteins. Proc Natl Acad Sci USA *109(47)*: 19408-19413, 2012.
59 Floyd SR, Pacold ME, Huang Q, Clarke SM, Lam FC, Cannell IG, Bryson BD, Rameseder J, Lee MJ, Blake EJ, Fydrych A, Ho R, Greenberger BA, Chen GC, Maffa A, Del Rosario AM, Root DE, Carpenter AE, Hahn WC, Sabatini DM, Chen CC, White FM, Bradner JE and Yaffe MB: The bromodomain protein Brd4 insulates chromatin from DNA damage signaling. Nature *498*: 246-254, 2013.
60 Martin M, Lefaix J and Delanian S: TGF-beta1 and radiation fibrosis: A master switch and a specific therapeutic target? Int J Radiat Oncol Biol Phys *47(2)*: 277-290, 2000.
61 Bhattacharyya S, Wu M, Fang F, Tourtellotte W, Feghali-Bostwick C, Varga J: Early growth response transcription factors: Key mediators of fibrosis and novel targets for anti-fibrotic therapy. Matrix Biol *30(4)*: 235-242, 2011.
62 Skwarchuk M and Travis E: Changes in histology and fibrogenic cytokines in irradiated colorectum of two murine strains. Int J Radiat Oncol Biol Phys *42*: 169-178, 1998.
63 Haston CK, Amos CI, King TM and Travis EL: Inheritance of susceptibility to bleomycin-induced pulmonary fibrosis in the mouse. Cancer Res *56*: 2596-2601, 1996.
64 Ohtsuka Y, Brunson KJ, Jedlicka AE, Mitzner W, Clarke RW, Zhang LY, Eleff SM and Kleeberger SR: Genetic linkage analysis of susceptibility to particle exposure in mice. Am J Respir Cell Mol Biol *22(5)*: 574-581, 2000.
65 Kleeberger SR, Bassett DJ, Jakab GJ and Levitt RC: A genetic model for evaluation of susceptibility to ozone-induced inflammation. Am J Physiol *258*: L313-L320, 1990.
66 Kleeberger SR, Levitt RC, Zhang LY, Longphre M, Harkema J, Jedicka A, Eleff SM, DiSilvestre D and Holroyd KJ: Linkage analysis of susceptibility to ozone-induced lung inflammation in inbred mice. Nat Genet *17(4)*: 475-478, 1997.
67 Hudak BB, Zhang LY and Kleeberger SR: Inter-strain variation in susceptibility to hyperoxic injury of murine airways. Pharmacogenetics *3*: 135-143, 1993.

Received December 12, 2013
Revised February 5, 2014
Accepted February 6, 2014